AD NUMBER

AD430298

NEW LIMITATION CHANGE

TO

Approved for public release, distribution
unlimited

FROM

Distribution authorized to U.S. Gov't.
agencies and their contractors;
Administrative/Operational Use; FEB 1964.
Other requests shall be referred to Office
of Naval Research, Washington, DC.

AUTHORITY

onr ltr 4 may 1977

UNCLASSIFIED

AD 430298

DEFENSE DOCUMENTATION CENTER

FOR

SCIENTIFIC AND TECHNICAL INFORMATION

CAMERON STATION, ALEXANDRIA, VIRGINIA

UNCLASSIFIED

DISCLAIMER NOTICE

THIS DOCUMENT IS BEST QUALITY PRACTICABLE. THE COPY FURNISHED TO DTIC CONTAINED A SIGNIFICANT NUMBER OF PAGES WHICH DO NOT REPRODUCE LEGIBLY.

NA-64-105

This research program is being conducted at the Los
Angeles and Rocketdyne Divisions, and is part of Project
DEFENDER under the joint sponsorship of the Advanced
Projects Agency, the Office of Naval Research, and the
Department of Defense.

DDC

FEB 25 1964

TISIA D
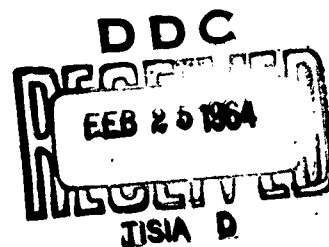
NORTH AMERICAN AVIATION. INC.

LOS ANGELES DIVISION
INTERNATIONAL AIRPORT
LOS ANGELES 9, CALIFORNIA

SPECTRAL EMISSIVITY OF FLASH COMBUSTION REACTION STUDY PROGRAM

SEMIANNUAL TECHNICAL SUMMARY REPORT

1 JUNE TO 31 DECEMBER 1963

CONTRACT NONR-4236(00)

NR012-505/4-24-63

PROGRAM CODE NO. 3730   1 JUNE 1963 TO 1 JULY 1964

Dr. J. M. Gerhauser, Principal Investigator

PREPARED BY

ENERGY CONVERSION &

ROCKETDYNE DIVISION

APPROVED BY

J. J. Pierro
Principal Scientist, Avionics

No. of Pages __48 + i and ii__   **REVISIONS**   Date __5 Feb. 1964__

DATE	REV. BY	PAGES AFFECTED	REMARKS

TABLE OF CONTENTS

LIST OF ILLUSTRATIONS

Section I

SUMMARY

The general objective of this study, as required by Contract NOnR-4236(00), is the investigation of the factors which control the duration, brightness temperature, and spectral distribution of radiant energy produced by chemical flashes. The program has been divided into four phases:

1. Development of test equipment.

2. Combustion studies.

3. Nonequilibrium studies.

4. Evaluation of data and system design.

During the period of 1 June to 31 December 1963, work has been expended in the first three phases, which will be presented in this report.

Major achievements of the period have been:

1. Disclosure of several chemical reactions which have theoretical flame temperatures greater than $5,000^\circ$K.

2. Achievement of a brightness temperature of $5,800^\circ$K with a zirconium-potassium perchlorate mixture.

3. Discovery of strong line emission in metal-potassium perchlorate reactions

4. Discovery of a very strong time dependency of line emission brightness during the progress of the reaction.

5. Theoretical prediction of intense nonequilibrium light emission from doped metal-oxidizer reactions.

6. Experimental verification of the predicted possibility of achieving intense line emission from a metal-oxidizer reaction by doping with metal salts.

Three of these achievements are considered extremely important to the present study. First, the $5,800^\circ$K temperature which was achieved is considered to be the highest temperature yet achieved in the United States with a pure chemical reaction. This high temperature indicates that even if nonequilibrium emission cannot be utilized, blackbody temperatures high enough to pump a laser are available from metal-oxidizer reactions.

Second, the theoretical prediction of nonequilibrium emission from doped metal-oxidizer reactions indicates that brightness temperatures considerably higher than $5,800^\circ$K are definitely possible. Work is now being performed to realize these possibilities.

1

Third, intense line emission from doped reactions indicates that non-equilibrium emission does exist in metal-oxidizer reactions during the initial stages of the reaction. Therefore, it is expected that extremely intense non-equilibrium emission will be achieved, as predicted by the theoretical non-equilibrium study, during the second half of the present study program.

Experimental studies will be continued in both combustion and non-equilibrium during the second half of the study period with strong emphasis on nonequilibrium. Three classes of dopants will be examined; namely, highly emissive metals, strong dipole salts, and high temperature fluorescent materials. Combustion studies will continue with stronger emphasis on basic reaction paths and production of excited species in the flame. This data will be used directly in the nonequilibrium dopant study. Thus, the final result of the two study areas will be the development of a source of high intensity nonequilibrium radiation.

Section II

EXPERIMENTAL EQUIPMENT

The necessary experimental equipment for a study of the light output of chemical flash reactions may be divided into three groups: Sensors, ignitors, and chambers. The sensors must measure light intensity as a function of time and wavelength. Two general types are in use. One type is used for producing time resolved spectra and the other type is used for measuring monochromatic intensities as a function of time. The calibration technique is discussed in detail because all temperatures quoted are accurate only insofar as the calibration is accurate.

The ignitor is used to ignite the reaction mixture at a predetermined time and with a minimum disturbance of the system. Therefore, a brief discussion of the ignitor design is presented.

The chambers in use may be divided into four types: Flat plate, atmospheric solid oxidizer, pressurized oxygen, and dynamic pressurization. Each is designed to provide a specific function for accurate intensity measurement at various specified conditions such as with pressurized oxygen, a solid oxidizer, or under high pressure. Consequently, a knowledge of a chamber design is important for an understanding of the data presented in section three.

TIME RESOLVED SPECTRA

The variation of light intensity from chemical flashes with wavelength and time can be measured by the use of the apparatus shown schematically in Figure 1. A Bausch and Lomb 1.5 meter grating spectrometer serves to record on film the light intensity incident on the entrance slit as a function of wavelength. Time resolution is accomplished by a sectored wheel revolving in front of the slit. At any particular time during the flash only a certain portion of the slit height is exposed to incident radiation by the sectored wheel. A sample sectored wheel is shown in Figure 2; this wheel has ten sectors each cut at a different radius. Each of the sectors shown occupies 18 degrees of arc of the wheel. Thus, for example, a wheel turning at one revolution in 40 milliseconds would allow a series of two millisecond exposures to be taken. Since the spectrometer is stigmatic, light from various portions of the slit height will be recorded at various corresponding heights on the film. To avoid the possibility of light being gathered from different portions of the radiating cloud leading to a confusion of spectral distribution of the light with a time distribution, the optics have been arranged so that the object image at the spectrometer slit is enlarged about three and one-half times.

A DC light source-phototransistor combination is used to measure the time per revolution as well as acting as a timing trigger for ignition of the chemicals- when the firing switch is flipped the ignition spark will be thrown the next time the phototransistor senses the light source through a slot in the sectored disk. Some of the light focused on the spectrometer entrance slit is deflected by beam dividers to two calibrated phototubes equipped with narrow band filters. The
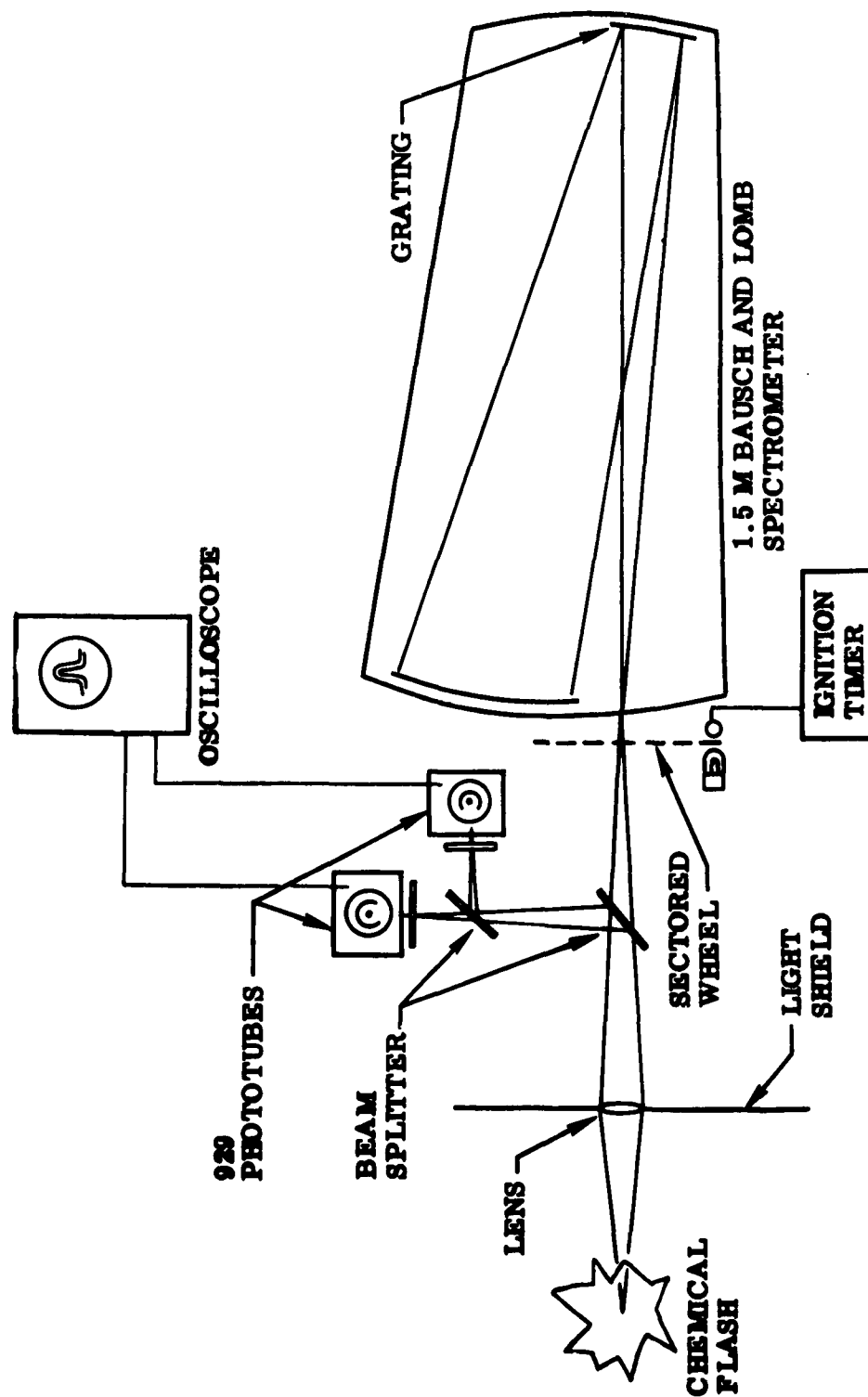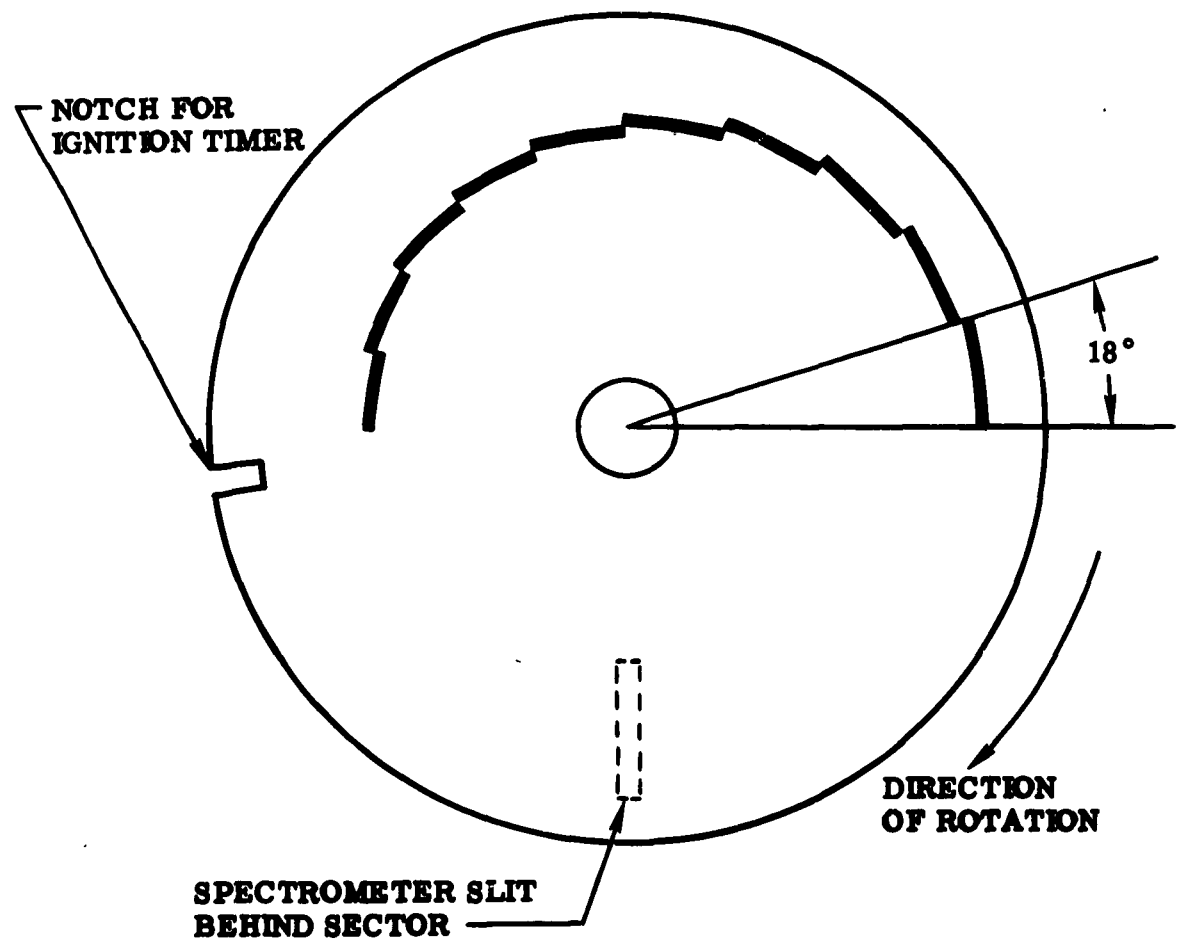
Figure 1. Radiant Energy Analyzer System

4

NOTCH FOR
IGNITION TIMER

18°

DIRECTION
OF ROTATION

SPECTROMETER SLIT
BEHIND SECTOR

Figure 2 . Sectored Wheel

output of the phototubes versus time is displayed on a C.R.T. and photographed.
Using the phototube output to measure light intensity and a microphotometer to
measure spectral film darkening versus time and wavelength, it is possible to
calibrate the film darkening with radiant intensity and hence brightness tempera-
ture. By careful duplication of the exposure time and developing technique, and
use of the same film emulsion batch number, the film can be similarly calibrated
at enough wavelengths to allow one to plot isotherms directly on any micro-
photometer trace of spectra taken in the same fashion. This seemingly complicated
system for calibrating film darkening versus radiant intensity is necessary
because of the reciprocity effect (1). The film must be calibrated using
identical exposure times as the exposure to be measured and available calibration
standards do not have a high enough radiant intensity to do the job.

Time resolved spectra should allow the rapid determination of brightness
temperature as a function of wavelength and time. This would be very helpful
in determining the effect of various additives on brightness or on the light
output in any narrow spectral region in the wavelength range of the instrument.
If nonequilibrium radiation can be produced, it is much more likely to be detected
by use of the spectrometer than by phototubes with narrow band filters. It is
also possible that the way in which intensity is observed to change with time
could reveal something about the combustion process.

MONOCHROMATORS

Measurement of light intensity in a given spectral region requires some form
of monochromator for selection of the spectral region. Several types of mono-
chromators have been tried in an effort to find a simple yet sensitive device.

One of the first methods tried was the use of Wratten filters. The Wratten
filters chosen were selected for narrow bandwidths and high transmittances in
the bandwidth. However, even the best Wratten filters had very wide bandwidths
($>500\text{Å}$) which produced anomalous results if the system under study deviated
greatly from a blackbody. Consequently, Wratten filters were scrapped.

After further study it was felt that interference filters would be the best
because they offered the advantage of narrow bandwidths ($<100\text{Å}$) and high
transmittance. Two types of interference filters are available:

1. The fixed type which is manufactured for a specific transmittance region.

2. The wedge type which transmits a given wavelength at a specific region
   on the filter.

Each type has found use in the laboratory. The fixed type has been used in
conjunction with the Bausch and Lomb spectrograph for calibrating the intensity
response of the photographic films. For this purpose it is admirably suited
because scanning is not necessary. Figure 1 shows use of these filters on the
time resolved spectra apparatus.

The wedge type is quite useful as a quick scanning device for rough plotting
of intensity distribution from flash reactions. It is extremely compact, and
may be easily calibrated because the spectrum is linear. Furthermore, it may be
mounted permanently to a phototube pickup box to construct a very small spectro-
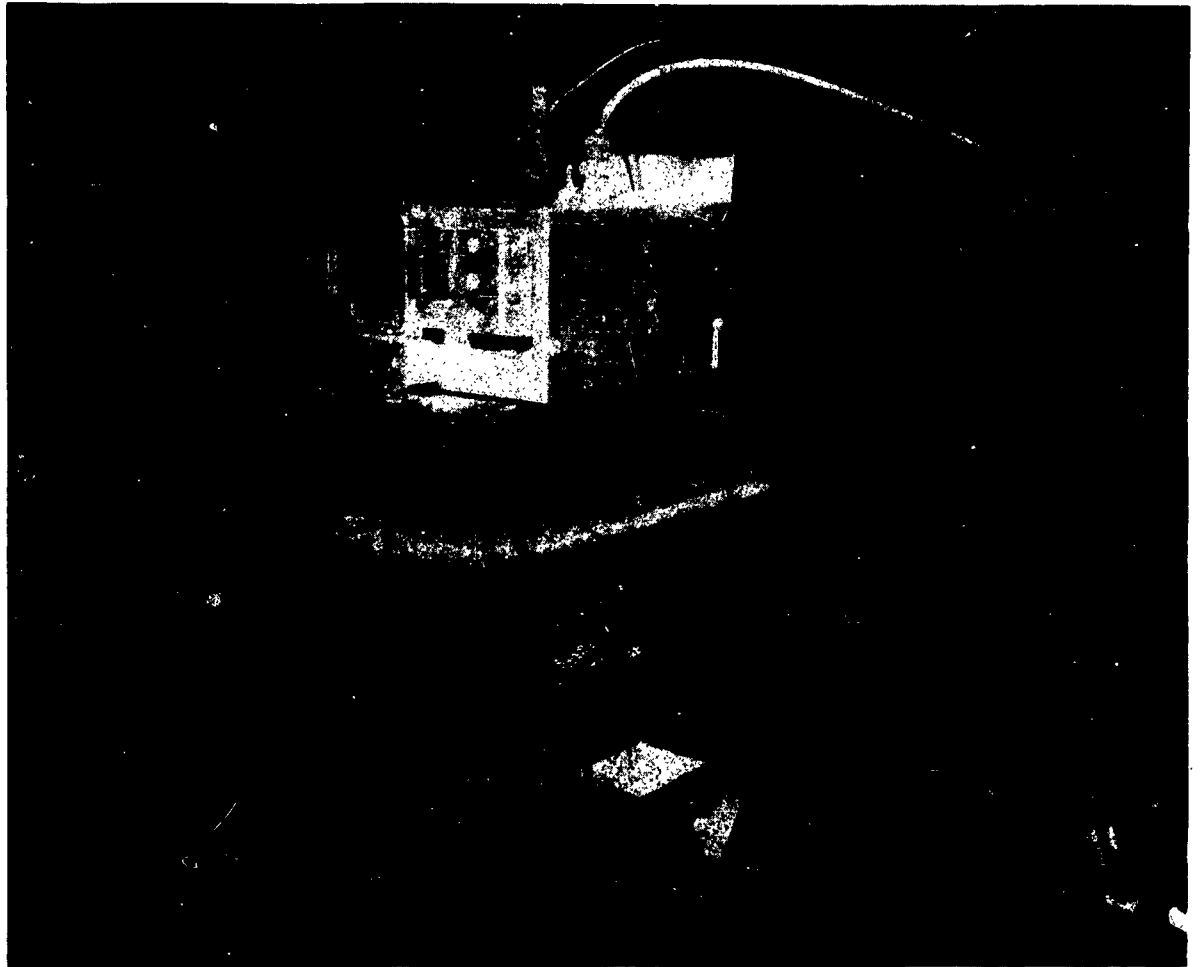photometer. Figure 3 shows the wedge filter mounted on a phototube box.

Figure 3. Phototube Spectrophotometer Sensor Unit

DETECTORS

Several types of detectors are currently in use in the laboratory. These may be divided into three categories: Solid state, photodiode tube, and photomultiplier. Each type is being used in its specific area of sensitivity.

The solid state photocells are currently in use in low sensitivity applications such as for pulse counters on the time resolved spectra setup. However, their high sensitivity in the infrared makes them admirably suited for measurements in the infrared. An infrared sensor is currently under construction which will utilize the solid state infrared detectors.

The photodiode tubes have been utilized in the visible range in conjunction with the wedge interference filters. Maximum sensitivity is at $5400\overset{\circ}{A}$.

The prime disadvantage of the photodiode tubes is that sensitivity is rather low when used with the wedge interference filters. Therefore, the minimum signal detectable above noise level corresponds to a blackbody temperature of approximately $2300^{\circ}K$.

For high sensitivity applications such as measurement of narrow line ($5\overset{\circ}{A}$) intensities in conjunction with the grating spectrographs, photomultiplier tubes are used. These tubes offer the advantage of extremely high sensitivity, but are subject to microphonic pickup. For this reason, the photomultiplier tubes are not in more general use in the laboratory.

SYSTEM CALIBRATION

Accurate measurement of absolute light intensities requires an accurate system calibration. Before a system calibration can be undertaken, suitable intensity standards must be chosen.

As a primary standard, a tungsten ribbon bulb calibrated by the National Bureau of Standards was chosen. Because it was necessary to preserve this standard, several tungsten ribbon bulbs were calibrated against the primary standard to serve as expendible secondary standards. At the time of calibration of these secondary standards, an optical pyrometer was also calibrated for use as a cross check on the decay rates of the secondary standards. Thus, as the secondary standards are used, they may be continuously recalibrated with the optical pyrometer. In actual operation, however, recalibration was not necessary until the filament approached burnout. It was assumed that the pyrometer calibration did not decay because the calibration had remained unchanged during a two year period of use prior to use in the laser laboratory. A second calibration of the pyrometer in the laser laboratory after six months operation has confirmed this assumption.

To eliminate random errors in calibration, the radiant intensity of two secondary standard bulbs was calculated at several operating temperatures by use of the tungsten emissivity tables and the blackbody radiation tables prepared by the National Bureau of Standards. Cross check with the original calibration gave no significant errors, therefore, the tables were assumed correct for the two bulbs in question.

Because random errors could occur during system calibration, the system was calibrated at several bulb temperatures between $2,200^{\circ}K$ and $3,000^{\circ}K$ to give

NA-64-105

statistically significant calibration curves. The actual response curves were found to be linear with intensity as was originally assumed. Figure 4 shows the normalized calibration curves plotted for one of the wedge interference filters and 929 phototubes currently in use in the laboratory. A similar calibration procedure was used on all sensors currently in use.

Calibration of film response used in the grating spectrographs is performed during each shot by measuring the radiant intensity at three or four selected spectral regions with interference filters plus 1P28 photomultiplier tubes. With this data isotherms may be plotted on the microdensitometer readouts to assist in determination of film response.

Brightness temperatures found by use of the present calibration techniques are accurate to $\pm$ 2 1/2 per cent up to 6000°K. Higher temperatures will require a higher temperature standard source for accurate calibration.

DEVELOPMENT OF IGNITION SYSTEM

The ignition of metal-oxidizer mixtures requires that some of the metal be raised to its boiling point before autocombustion can begin. Because it was desired to measure the temperature of the chemical reaction, and not the ignition temperature, a second requirement was that the ignition energy must be much less than the available reaction energy. Third, sensing and recording equipment to be used required synchronization of the flash with the recording period. Therefore, some form of electrical ignition with a very short delay was necessary.

The first attempts at controlled ignition were performed with Pyrofuze triggered by a battery. Ignition was erratic, often occurring several seconds after the electrical impulse. Furthermore, rapid firing in sequence was almost impossible.

A second approach was to use an exploding wire triggered by a high voltage capacitor discharge. Ignition occurred almost instantaneously, but again rapid firing was almost impossible.

Spark discharges were tried next, but ignition was erratic, apparently because of a low current density. However, rapid firing could be easily accomplished if the erratic behavior could be corrected.

To increase current densities, a capacitor discharge was used. Ignition was uniform and instantaneous in all fixtures tried. The wire electrodes used initially were easily jarred from alignment and were vaporized very quickly. Therefore, only two or three firings could be made before the electrodes had to be replaced.

To solve the electrode problem a search was made for more rigid electrodes. Automobile spark plugs proved suitable. The base of the plug was filled with epoxy resin to provide a flat surface for the pyrotechnic powder.

Control of the capacitor discharge circuit was first tried by using a mercury thyratron. However, a large leakage voltage was always present across the electrodes which could cause premature ignition. The thyratron was replaced with a high voltage, heavy duty double pole relay which provided complete isolation of the electrodes until actuation.

The final ignition circuit and its operating behavior is shown in Figure 5.

NA-64-105

Figure 4 . Photocell + Interference Filter Calibration

10

NA-64-105

110V AC

3KV TRANSFORMER   RECTIFIER   VOM   0.25 UFD CAPACITOR   RELAY   ELECTRODE

MILLIVOLTS

REACTION SPIKE

IGNITION SPIKE

1-10 MSEC

100 μ SEC

TIME

TYPICAL PULSE BEHAVIOR
FROM OSCILLOSCOPE TRACE
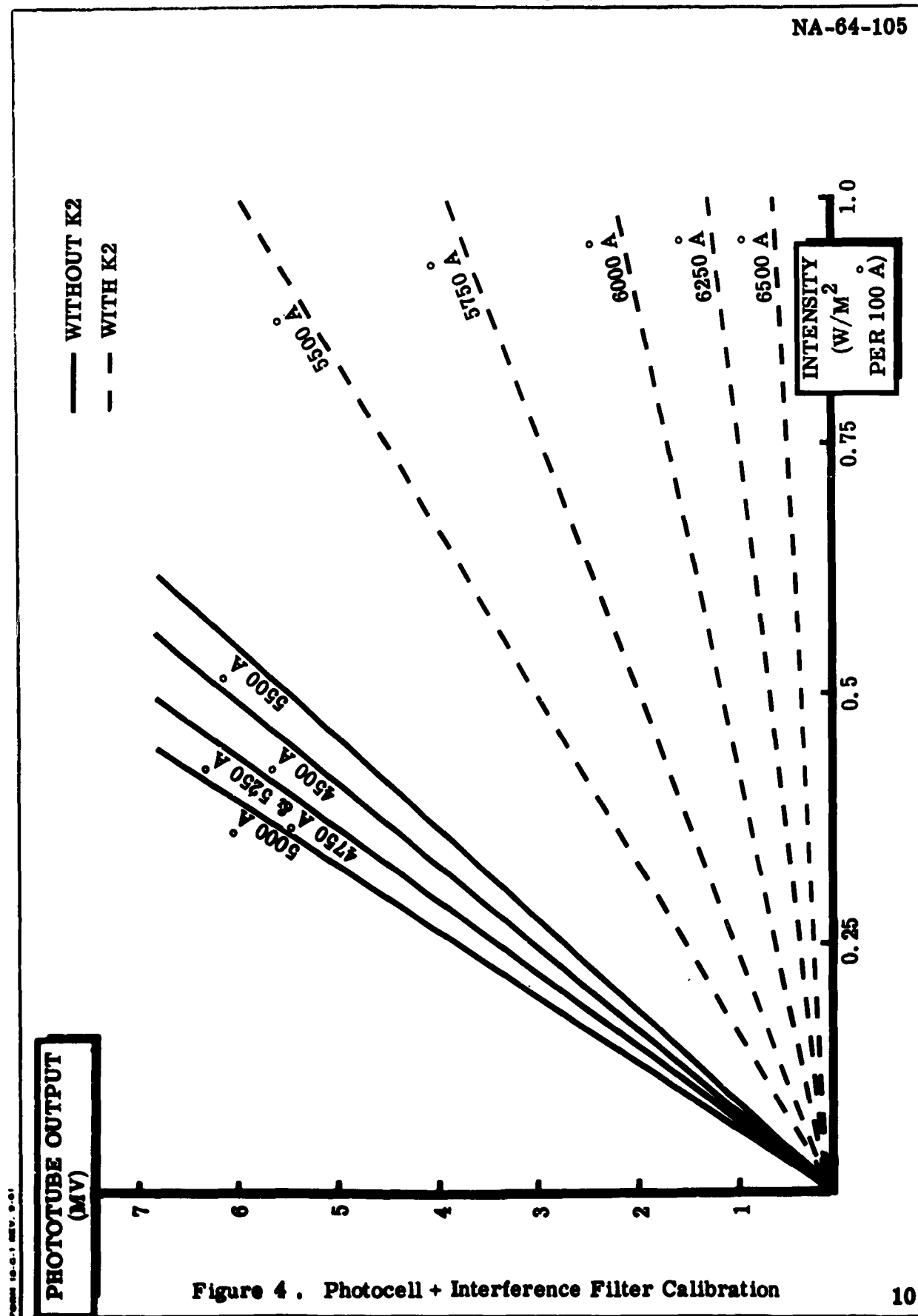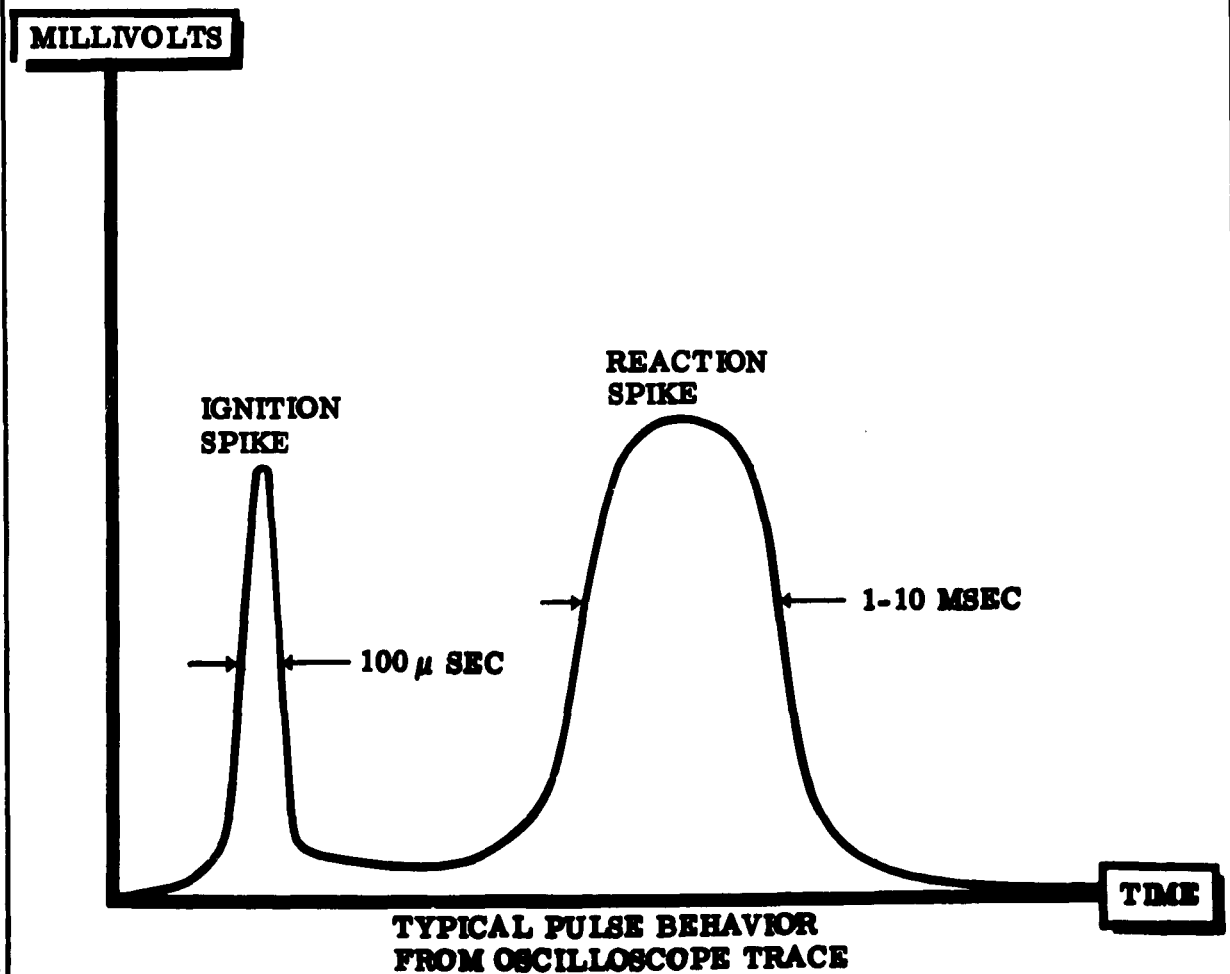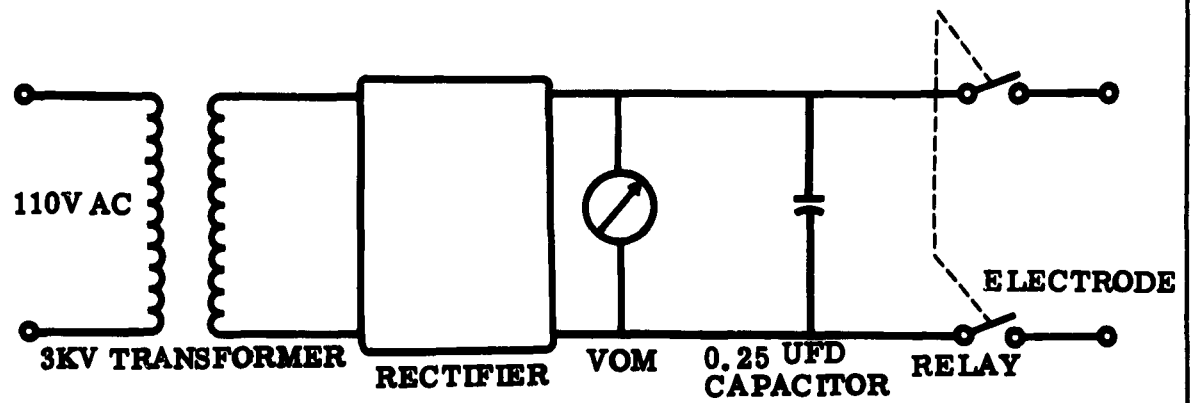
Figure 5 . Ignition Circuit

11

DESIGN OF CHAMBERS

Chamber design is perhaps the most important variable affecting temperature measurement of pyrotechnic flashes. Consequently, very careful thought has been given to the design of special chambers to insure accurate temperature measurement.

One of the first designs tried is the simplest. It consists merely of a flat metal sheet upon which the flash mixture is ignited. In general a hemispherical fireball is formed. The flat sheet design provides for minimal pressure and shock effects while allowing complete access to the flame. The prime disadvantage is that rapid cooling occurs at the outer surface of the fireball which produces a zone of line reversal and scattering, thereby giving optical temperatures somewhat lower than the true temperature. A second disadvantage is that fireball size is uncontrolled and varies greatly between shots.

To alleviate some of the problems associated with the flat sheet, the atmospheric omnidirectional chamber was designed. This design controls the size and shape of the fireball by directing it upward through a short chimney equipped with a 360° window at its base. Measurements are made near the base of the fireball at a point where the size is relatively constant for each shot. The greatest disadvantage is that large eddy currents are set up in the apparatus during firing which circulate a large amount of dust into the field of view. Thus, scattering of emitted light becomes a serious problem.

The final atmospheric chamber design resulted when the omnidirectional chamber was modified to correct the scattering problem. An adapter was designed to fit the omnidirectional chamber which would highly collimate the flame and sent it through an overexpanding nozzle to bring the flame to one atmosphere pressure. Slightly downstream, a 1/2 inch window was placed for a view of the center of the flame. With this adapter, eddy currents developed downstream from the window, thus correcting the smoke scattering problem. Intensity variations of approximately five per cent were observed between successive shots, but this could be attributed mainly to variations in powder mixing. See Figure 6 for the final design of the atmospheric solid oxidizer chamber.

Studies with pressurized oxygen placed these stringent requirements on chamber design:

1. Chamber must be completely sealed.

2. Chamber must be inert to high pressure oxygen.

3. Chamber must withstand shock loading.

4. Chamber must have sufficient volume to prevent excessive pressure buildup.

5. Chamber must be equipped with a window capable of withstanding maximum pressure of chamber.

6. Chamber must be equipped with an ignitor capable of withstanding maximum chamber pressure and 3,000 volt capacitor discharge.
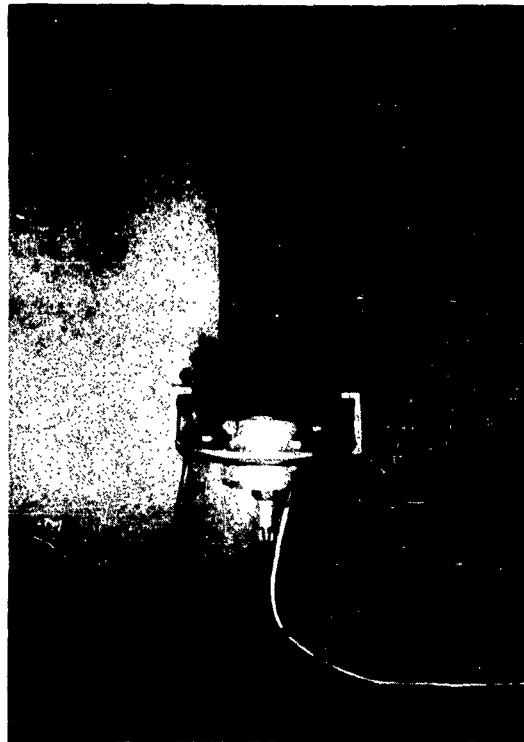
ASSEMBLED
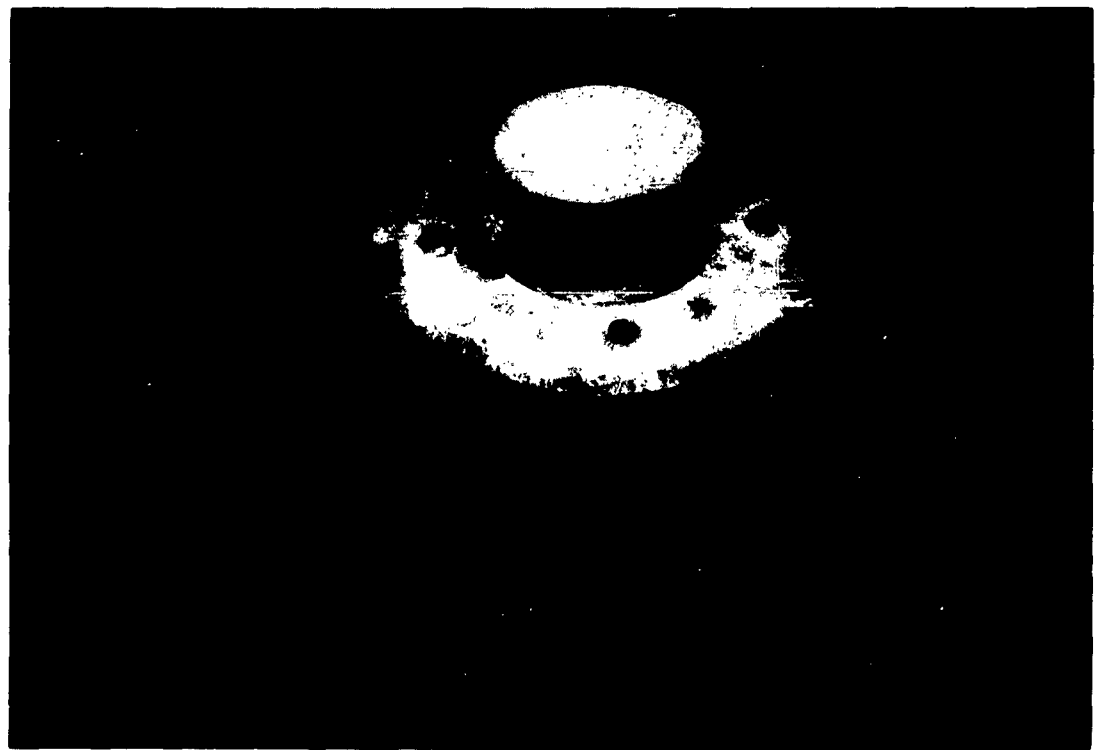
INTERIOR VIEW

Figure 6 . Atmospheric Chamber

13

The final design of the pressurized oxygen chamber based on these requirements is shown in Figure 7.

A dynamic pressurization chamber was designed to allow measurements at extremely high pressures ($>10^4$ psi). Design criteria were:

1. Provide for containment up to 10^5 psi.

2. Electrical ignition of charge.

3. Transparent window for viewing.

The chamber is shown in Figure 8.

NA-64-105

ASSEMBLED

DISASSEMBLED

Figure 7 . Static Pressurization Chamber

ASSEMBLED

DISASSEMBLED

Figure 8 . Dynamic Pressurization Chamber

16

Section III

COMBUSTION STUDIES
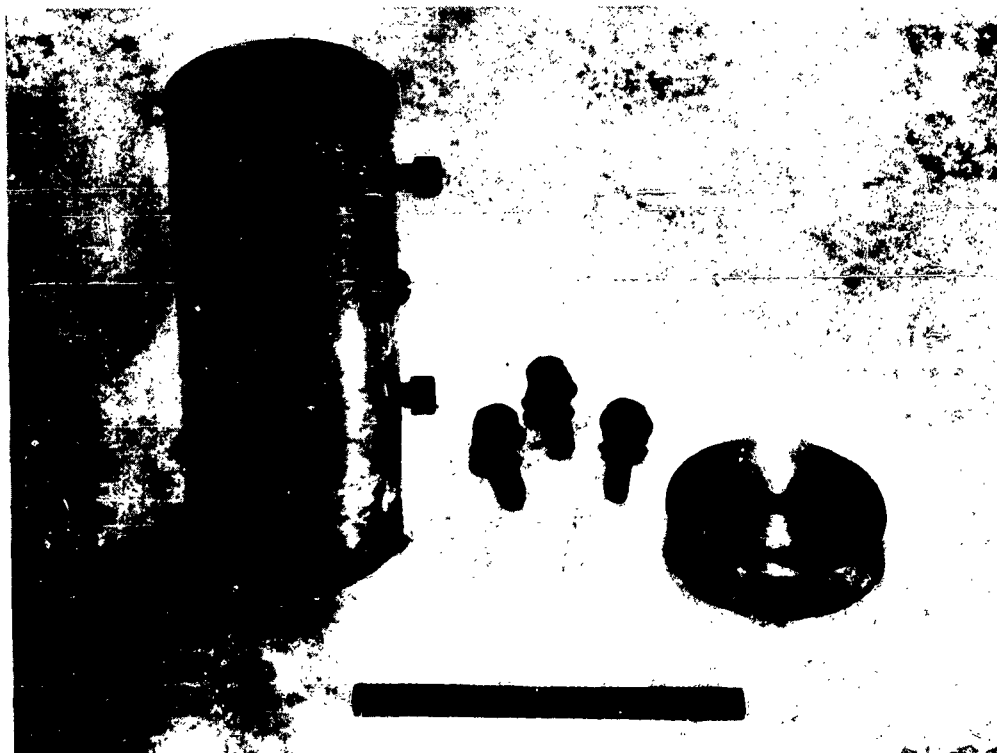
Before an experimental study of nonequilibrium radiation from chemical reactions can proceed, accurate knowledge of the equilibrium behavior is necessary. The primary variable to be measured at equilibrium is the flame temperature of the reaction. Knowledge of the flame temperature is important because, by defini- tion, nonequilibrium radiation is at an effective temperature higher than the flame temperature. Therefore, to determine experimentally whether emission observed in a spectral region is equilibrium or nonequilibrium, the temperature observed must be compared with the actual flame temperature.

Measurement of the flame temperature by optical methods requires measurement of the brightness temperature and emissivity of the flame in an equilibrium emission region. These measurements are the basis of the combustion study being performed under the present contract. In the combustion study, it is desired to completely characterize the emission behavior of the basic combustion reactions so that when dopants are added the change in the emission spectrum and its magni- tude may be instantly known.

Another goal of the combustion study is to locate chemical reactions which produce extremely high temperatures. The importance of high temperature reactions is that in these reactions, the available energy is a maximum. Thus, there is a greater chance of success in the use of nonequilibrium dopants in these reactions.

To serve as a guide for choice of high temperature reactions, a theoretical adiabatic flame temperature calculation was made for several reactions. The highest temperature reactions were selected for experimental study under various conditions. The theoretical and experimental results are presented here to serve as a basis for understanding the problems associated with the nonequilibrium study presented in Section IV. The highest temperature obtained during test was a 5800°K temperature at 5500Å as shown in Figure 13.

THEORETICAL ADIABATIC FLAME TEMPERATURE

An adiabatic flame temperature is the calculated temperature for equilibrium conditions for a flame in which no energy is lost to the surroundings. The calculation of equilibrium conditions is rather lengthy, but programs for com- puters have been written to do the calculation.

In the calculation of equilibrium, a table of possible compounds is searched and those compounds that are thermodynamically preferred are used to obtain the solution. It is obvious that the accuracy of the calculation is dependent on the input thermodynamic data. For the systems calculated (except hafnium) the JANAF thermodynamic data is used. The difference in input data probably accounts for the difference in quoted temperatures.

From the heat of formation of the oxide, it is expected that thorium, the rare earths, hafnium, zirconium, beryllium, and aluminum will give the hottest flames. Some of the adiabatic temperatures calculated by this method are shown

in Figure 9. It should be noted from these graphs that increasing pressure does not raise the temperature as much as might be expected since at these high temperatures most of the energy is being stored in molecular vibrations. The data for thorium and the rare earths is not available, but it is expected these should also give high flame temperatures with the possibility that the rare earths may emit in their absorbtion bands and thus permit matching of the flame emission spectrum to the laser absorbtion spectrum.

COMBUSTION STUDIES

Preliminary Experiments - To facilitate checkout of equipment, it was decided to search for a basic reaction which was easy to handle and produced reproducible flashes. After checking several possible reaction mixtures, it was found that a mixture of 1/5 magnesium, 1/5 aluminum, and 3/5 sodium chlorate gave the desired results. This mixture was stable for long periods, easy to ignite, burned in less than ten milliseconds, and produced brightness temperatures close to the calibration temperatures used. Also, even after long storage, the intensity varied by less than five per cent from shot to shot.

To record short pulses, a techtronix 535 oscilloscope was found suitable when equipped with a Polaroid oscilloscope camera. If necessary, two channels could be recorded simultaneously. Triggering was accomplished by adjusting the scope to trigger off the ignitor spike which occurs just before the chemical flash.

An intensive experimental study of possible errors was conducted with the basic reaction mixture. From this study, several sources of extraneous signals were found and eliminated. First, extensive masking of the reaction chamber was necessary because of the formation of a large luminous cloud above the atmospheric chamber during firing. Second, large signals from the room lights necessitated operation in the dark. Third, various signals were picked up from electrical equipment in operation in other areas of the laboratory if the output cables from the sensors were not well shielded. Fourth, the recording equipment was sensitive to shock waves produced by the faster flashes.

Experimental Measurements - After the preliminary experiments were completed and the system was completely checked out, an intensive study of brightness temperature variations with wavelength was undertaken. Several solid oxidizer metal mixtures were examined including:

$$Mg \; + \; Al \; + \; NaClO_3$$

$$Mg \; + \; Al \; + \; KClO_4$$

$$Zr \; + \; KClO_4$$

$$Hf \; + \; KClO_4$$
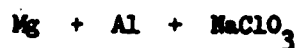
All reactions except hafnium plus potassium perchlorate indicate a large increase in brightness temperature towards the red end of the visible spectrum as shown in Figure 10. Several explanations for this phenomenon have been suggested, all of which are based on Mie or Rayleigh scattering of light from dust clouds. However, the brightness temperature behavior in the infrared will be necessary before a reasonable explanation can be found.

18

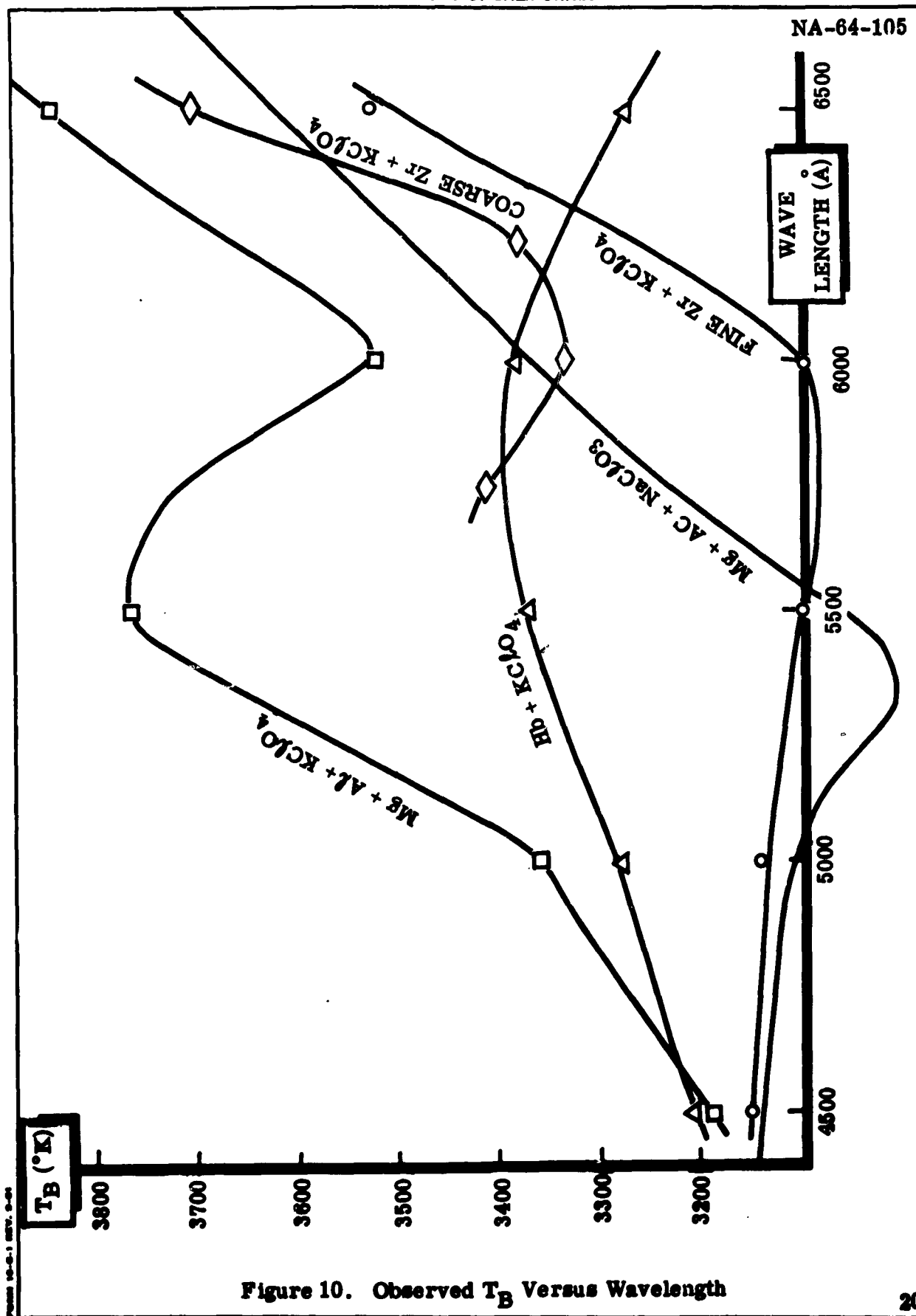Figure 9. Theoretical Adiabatic Flame Temperature Versus Pressure   19
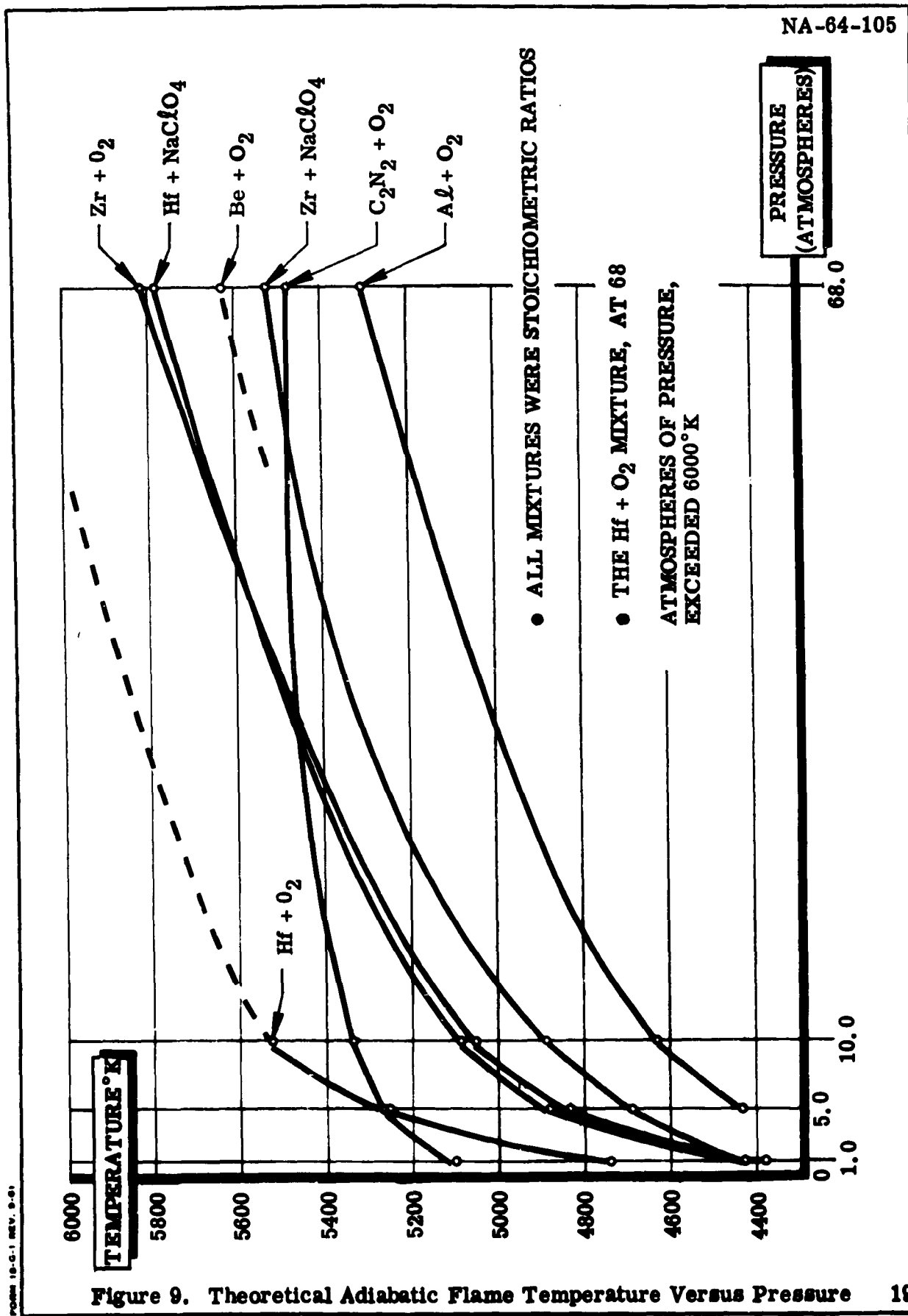
Figure 10. Observed T_B Versus Wavelength

Reaction time profiles vary greatly depending on the mixtures used. A strong correlation was found between initial metal powder size and reaction duration. In general, the finer meshes produced shorter reactions as expected, however, little correlation was found between mesh size and brightness temperatures. With zirconium, the coarse powder resulted in higher temperatures than the fine mesh powder. This effect may be due to the presence of an oxide layer on the powder which would effectively reduce the free metal concentration in the finer powders because of the larger surface areas present.

Studies with pressurized oxygen were undertaken to verify the theoretically predicted adiabatic flame temperatures. At first, the metal powders were used directly, but the variation of brightness temperature with pressure always indicated a maximum. This effect was caused by the fact that only at one pressure would the system be stoichiometric. This effect is shown with aluminum powder in Figure 11. Hafnium and zirconium behave similarly.

To correct the stoichiometry problem studies were initiated with metal wool packed into pyrex retainer tubes. The results with aluminum wool are shown in Figure 12 with the theoretical falme temperature plotted above. If an emissivity of 0.225 is assumed for the aluminum reaction, the "actual" flame temperature is found to agree quite closely with the predicted flame temperature.

As a check on this approach, zirconium-potassium perchlorate mixtures were fixed under oxygen pressurization. The results are shown in Figure 12. Again, if the emissivity is assumed to be 0.0816, fair agreement is found between the "actual" flame temperature and the predicted flame temperature.

Zirconium-oxygen reactions are currently under study, but no results are available at present. However, it is assumed that similar behavior will be observed.

It should be mentioned that these experimental emissivities are subject to large errors if the theoretical flame temperature are in error, or if smoke obscuration of the reaction zone is significant. Furthermore, the two path measurements taken on the special apparatus set up for emissivity measurement indicates that the emissivities are actually near 0.7. However, these measurements are also subject to smoke obscuration and are probably higher than the actual emissivities. Again, infrared measurements will be extremely useful for determining the actual flame temperature. When infrared data is available, which will be very soon, the actual flame emissivities will become available.

Higher brightness temperatures were expected with an increase in pressure. To explore the high pressure region, measurements were taken with solid oxidizer-metal mixtures in the dynamic pressurization chamber. Pressures up to 10^5 psi could be handled in the chamber. Extreme difficulty was experienced in conducting these high pressure tests for several reasons. First, conditions could by no means be duplicated between successive shots. Second, the window sometimes ruptured, nullifying data received. Third, flying fragments from the ruptured window required elaborate protective screens. Fourth, the short duration pulses were hard to record because of large variations in the induction period between the ignition pulse and the combustion pulse. Nevertheless, significant data was obtained on many shots and are summarized in Table I . The pressures reported are very approximate and were found by calculating the pressure necessary to repture the window. A typical reaction intensity versus time plot is shown in Figure 13.

NA-64-105
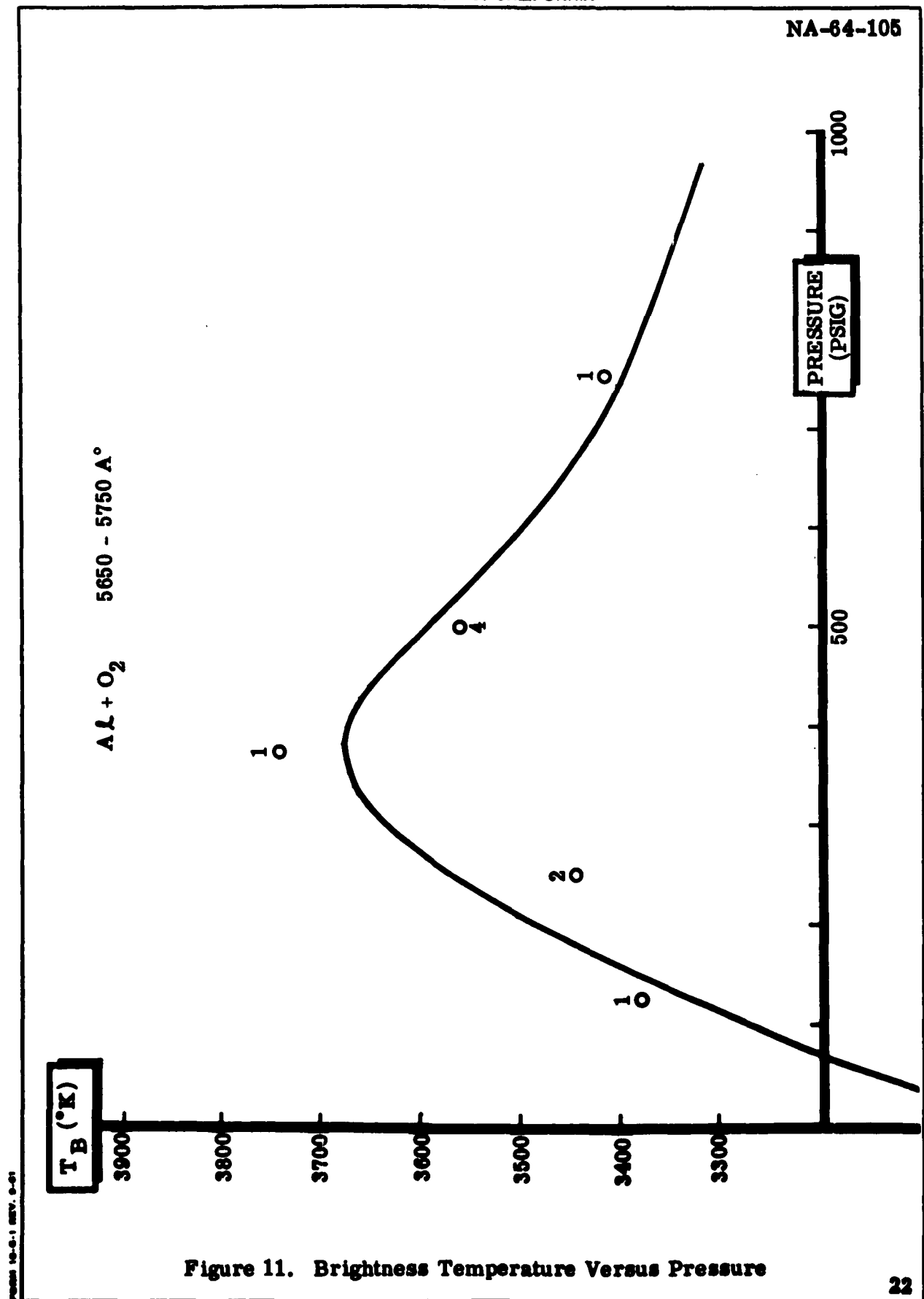
Figure 11. Brightness Temperature Versus Pressure

22
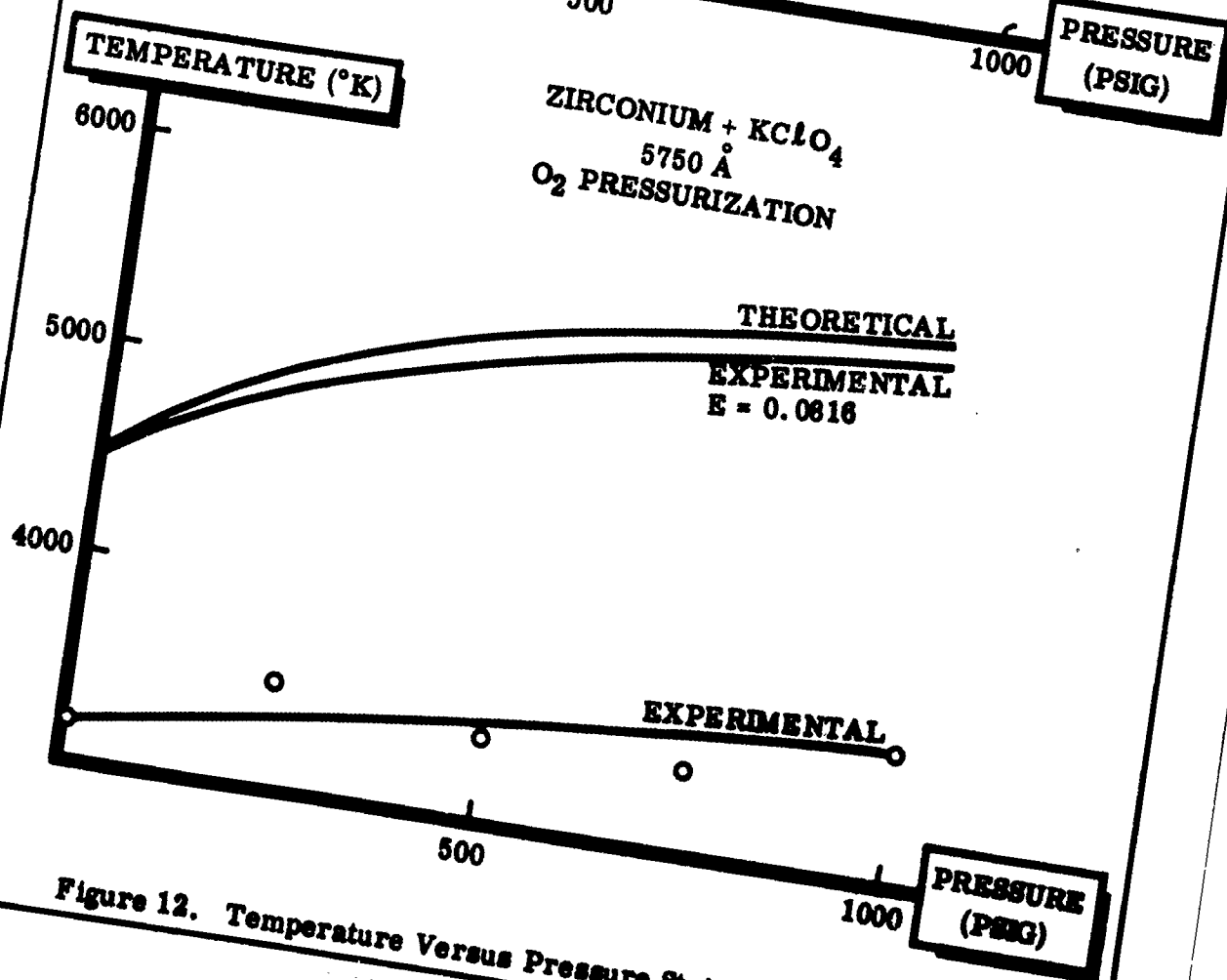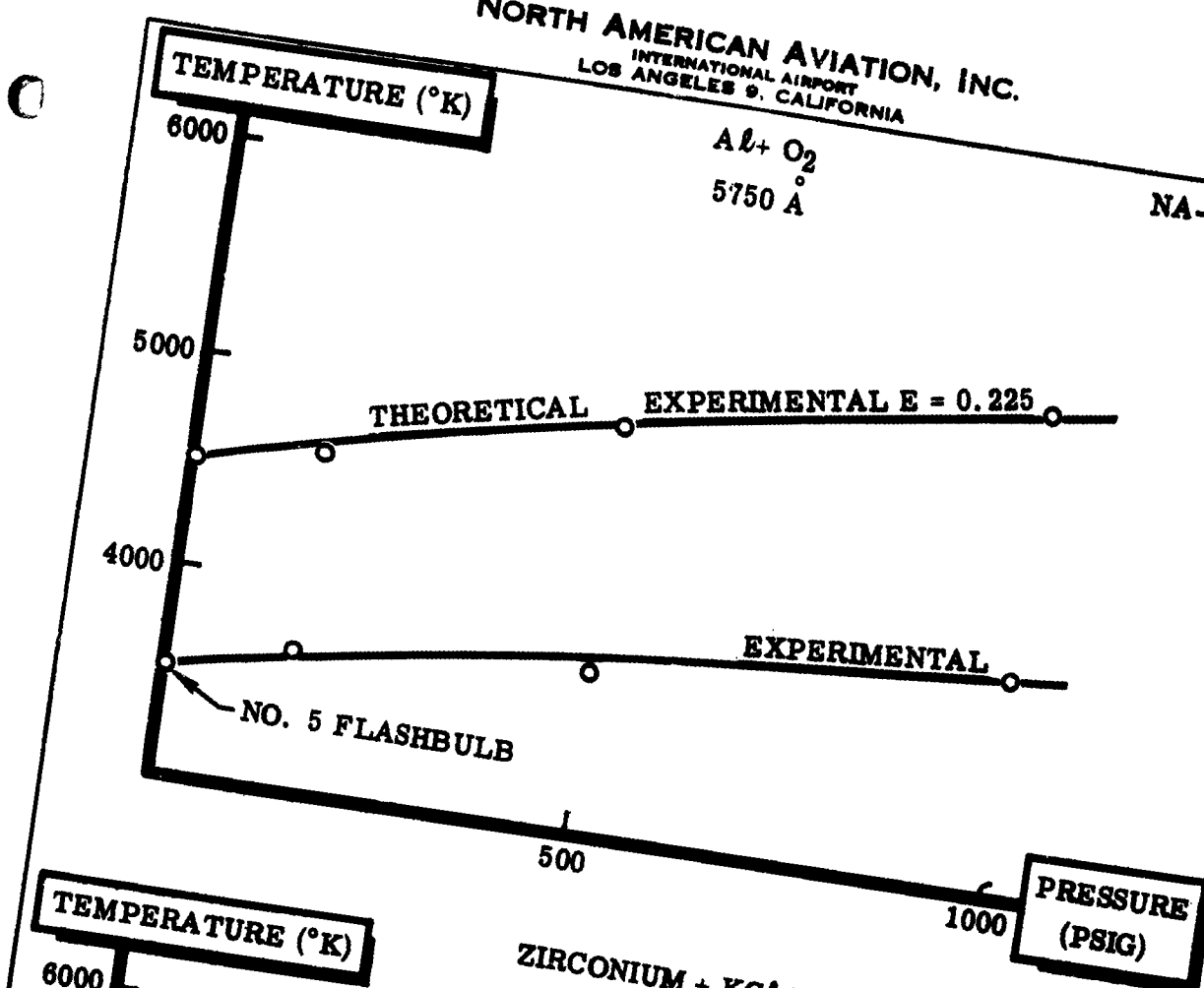
Figure 12.   Temperature Versus Pressure Stoichiometric System

23

NORTH AMERICAN AVIATION, INC.
INTERNATIONAL AIRPORT
LOS ANGELES 9, CALIFORNIA

Table I

DYNAMIC CHAMBER TEST RESULTS

Material	KIP/In.^{2}	Temp °K
$Al + Mg + KClO_4$	20	4150
$Hf + KClO_4$	20	4635
$Hf + Mn + KClO_4$	20	5270
$Zr + KClO_4$	80	5800

NA-64-105

1/8 IN. HOLE   1/4 IN. LUCITE WINDOW

$Zr + KClO_4$

5500 Å

11-14-63

PULSE TIME (MSEC)

TEMP (°K)

Figure 13.   Dynamic Pressurization Chamber

25

An effective way to increase the flame temperature of a reaction is to add extra energy to the reaction mixture. To accomplish this goal, it was decided to try an exploding wire in oxygen. Two types of wires were tried, aluminum and zirconium. The wire was exploded in a pyrex capillary tube under sufficient oxygen pressure to effect complete combustion. Just enough electrical energy was used to vaporize the wire. The results are shown in Figure 14 with a sketch of the tube used. The brightness temperatures observed were higher than the temperatures measured with the metal wool burning in oxygen. The saddles observed are caused by the condensation of metal oxide. From the observed brightness temperature and the calculated boiling point of the oxide, the emissivity may be roughly measured. The aluminum emissivity is approximately 0.26 and the zirconium emissivity is approximately 0.08. Therefore, the emissivities assumed in the pressurized oxygen studies are further substantiated.

Time resolved spectra have been taken of Al, Hf, Zr, and Nd reacting with $KClO_4$. Most of the time resolved spectra shots are of little value for brightness temperature determination because of lack of constant developer temperature, old developer, failure to operate the phototubes at the proper sensitivity range, change in film emulsion batch numbers, or an imperfectly cut sectored wheel allowing the various exposures to overlap slightly on the film. Only the most recently taken Al-$KClO_4$ shots are usable for film density versus brightness temperature calibration. The spectral region from 3500Å to over 6500Å covered by the spectrometer will eventually be calibrated at 4500, 5000, 5500, 6000, and 6500Å. A calibration for the 4500Å and 6000Å region is being prepared using Al-$KClO_4$ flashes and preliminary curves are shown in Figures 15 and 16.

In Figure 17 the microphotometer traces of a series of spectra are shown. In it one can see the progression of the flash reaction at two from Al, K, and Na (an impurity in the $KClO_4$) vapor. The bands of AlO and the continuum radiation of solid and liquid phases are not as yet detectable. Perhaps the most striking occurrence is the increase in continuum brightness temperature in the blue region of the spectrum before the continuum in the red can be detected (2-4 milliseconds). The intensity of the NaD lines is already quite high. Differences in film response to blue and red light, therefore, cannot account for this discrepancy; apparently, continuum emissivity is initially higher towards the blue end of the spectrum. During the same 2-4 millisecond time, the AlO bands at 5079Å and 5337Å are not yet visible while those at 4648Å and 4842Å appear quite intense. Because the sensitivity of Kodak 103F film is lower in the green, and this region has not as yet been calibrated, it is possible that failure to pick up the AlO bands at 5079Å and 5337Å is attributable to the lower film sensitivity. At subsequent time intervals the microphotometer traces show an increase in continuum, band, and line radiation; K lines and the center of the NaD-lines are observed in absorption, but AlO is always present in emission. Either the gas is hotter than the solid, i.e. Al is oxidized primarily in the gas phase, or the emissivity of the solid is lower. From the preliminary film density calibration data gathered thus far, it appears that the continuum brightness temperature in the 4500Å region is always greater than in the 6000Å region and is more comparable to the peak brightness temperature of the NaD-lines (even though these lines are self absorbed near their centers). This would indicate that the particles and the gas are at about the same temperature and the emissivity of the particles is higher at 4500Å than at 6000Å. More can be said about the Al-$KClO_4$ system when calibration of the film is completed.
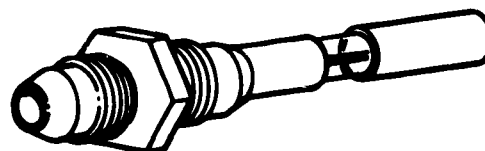
O$_2$ AT 500 PSI

STOICHIOMETRIC RATIO
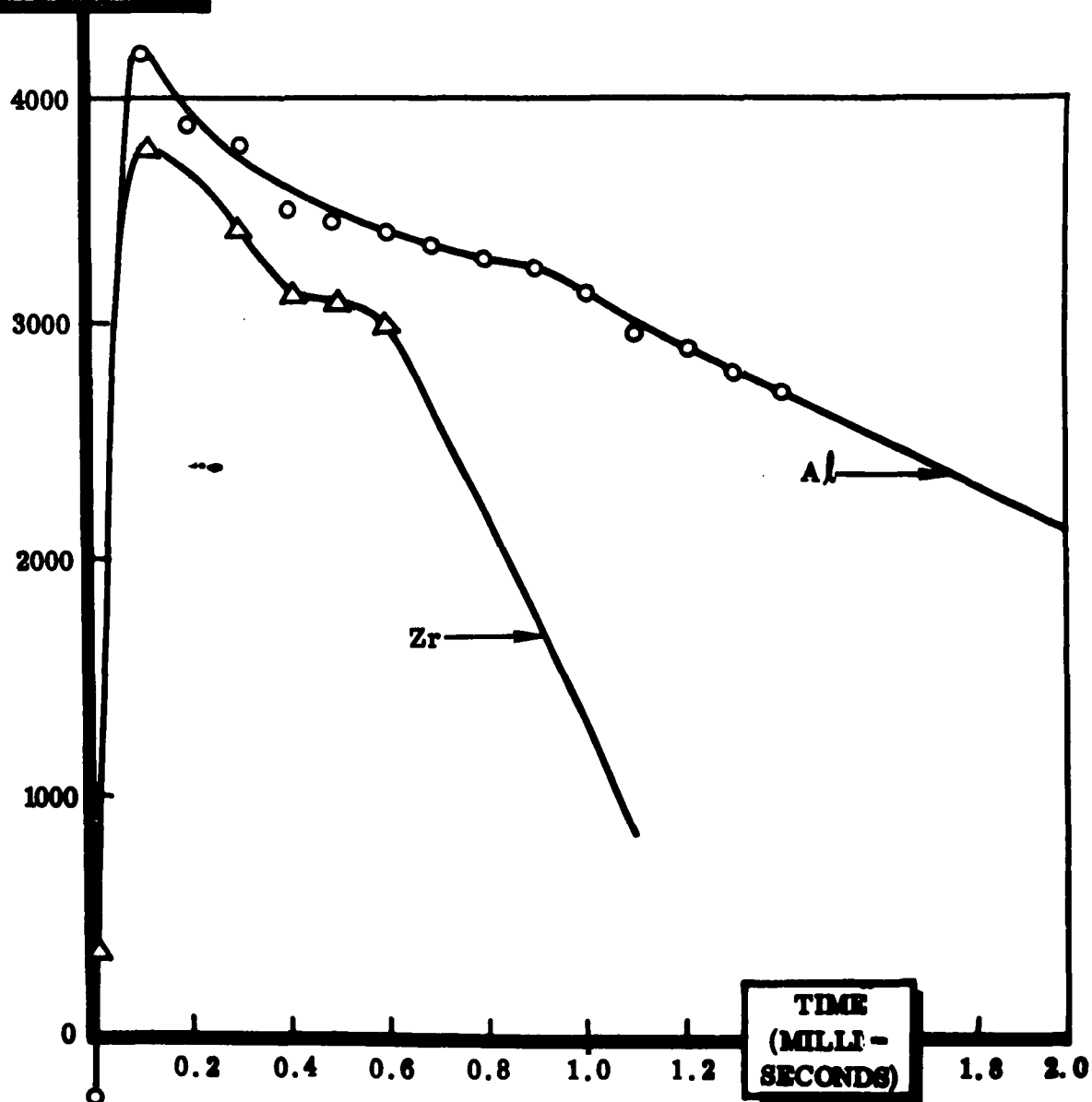
Figure 14. Exploding Wire Chemical Reactions

27

Figure 15. Percent Light Transmission Versus Phototube Output

28
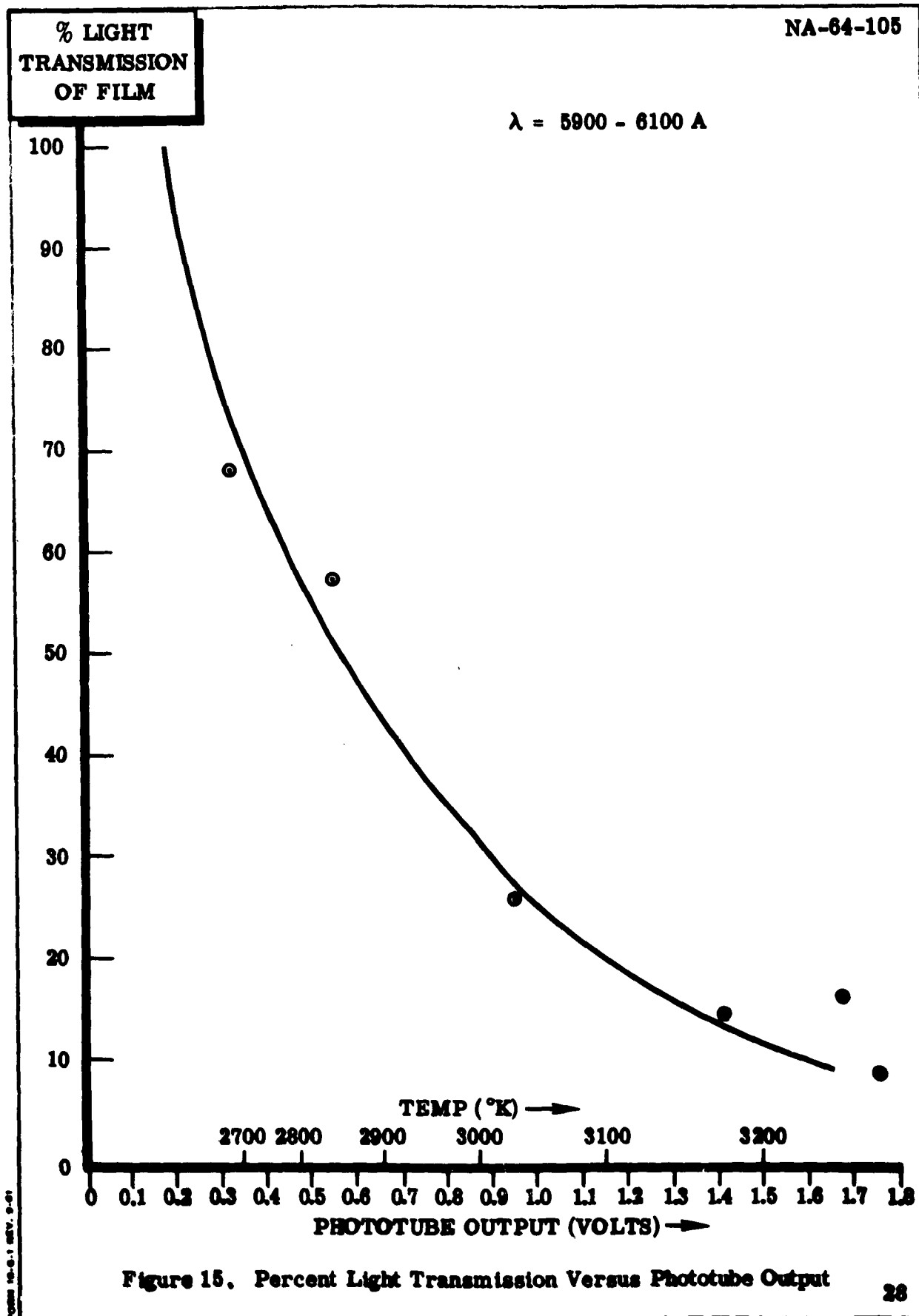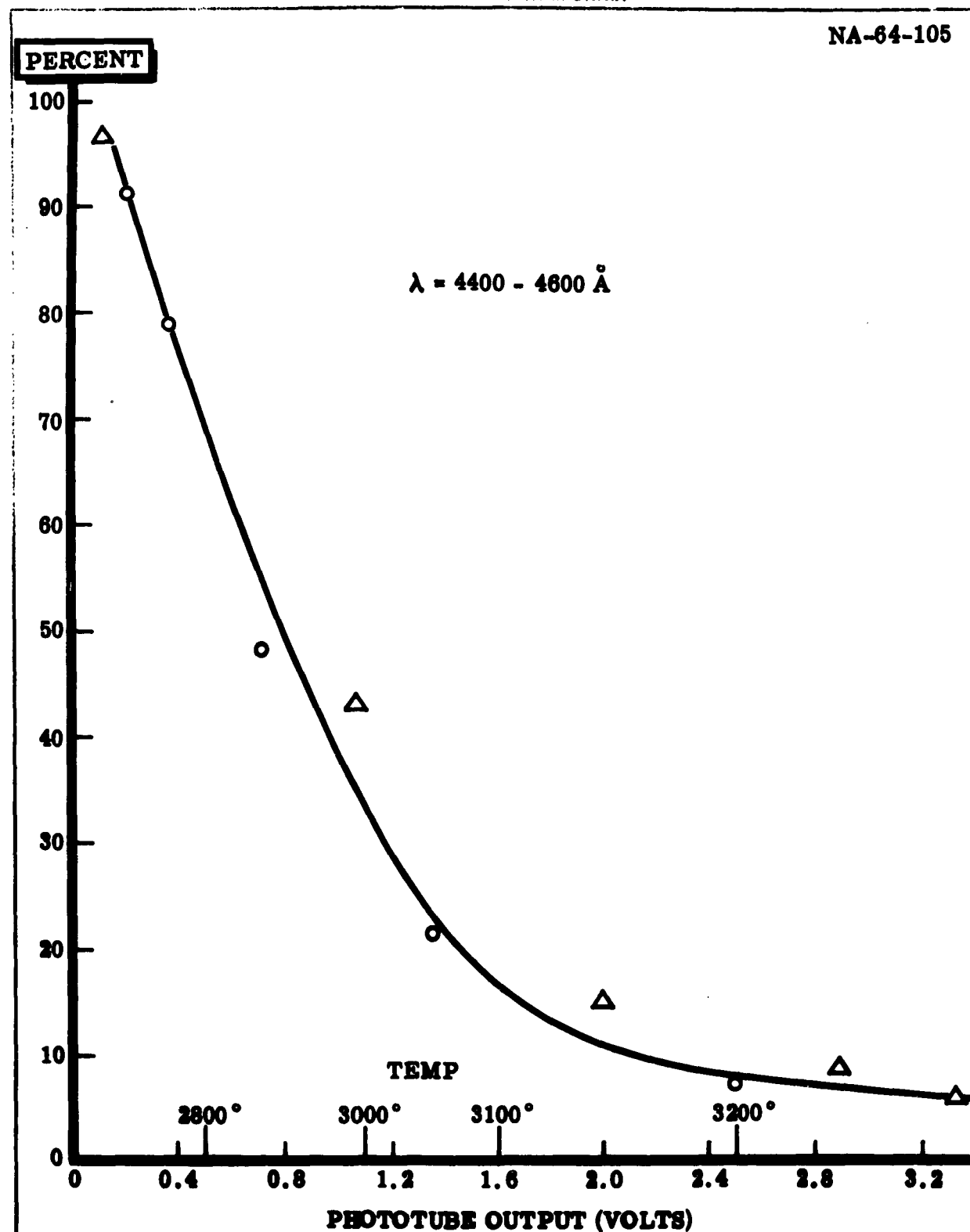
Figure 16. Percent Light Transmission Versus Phototube Output
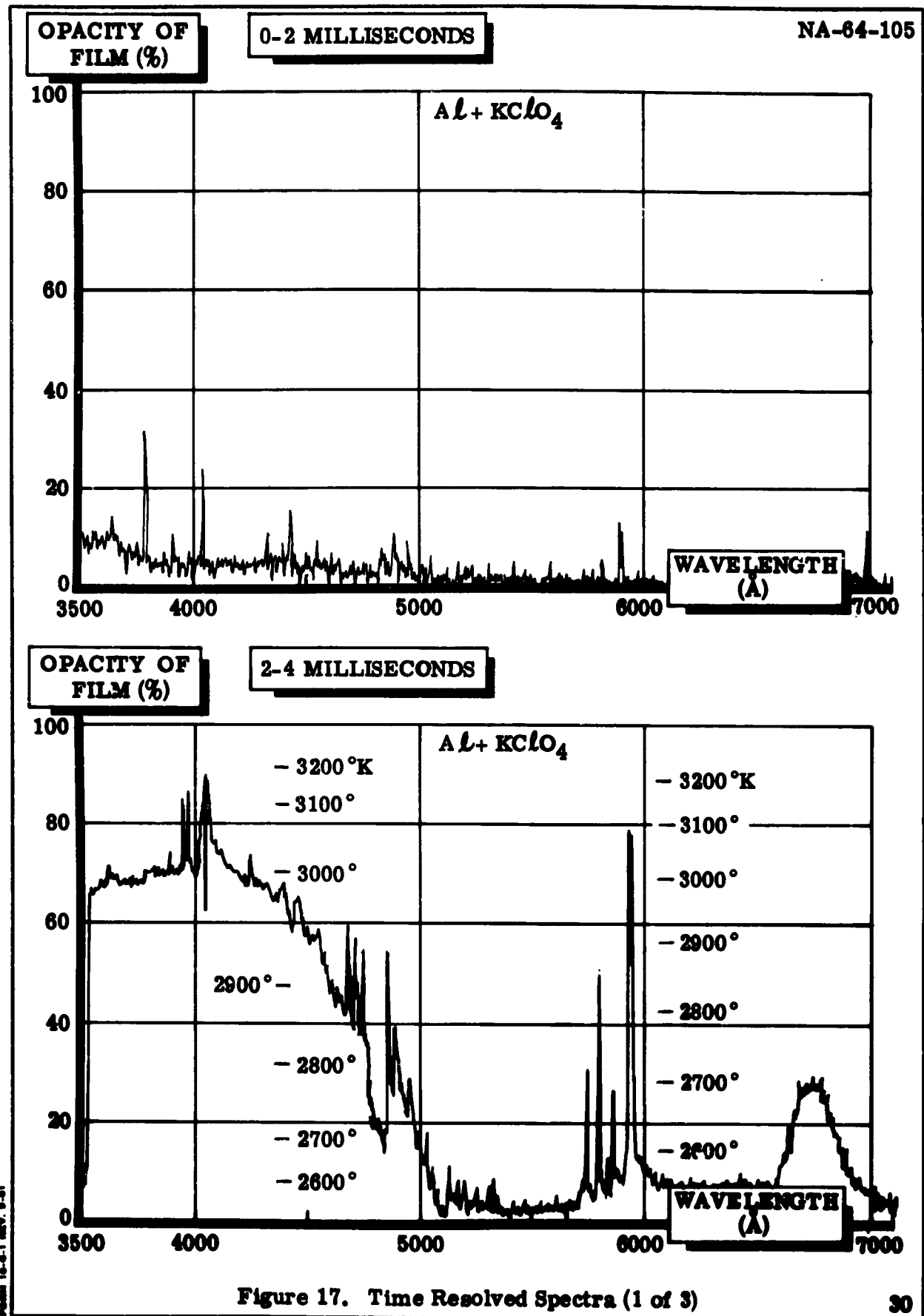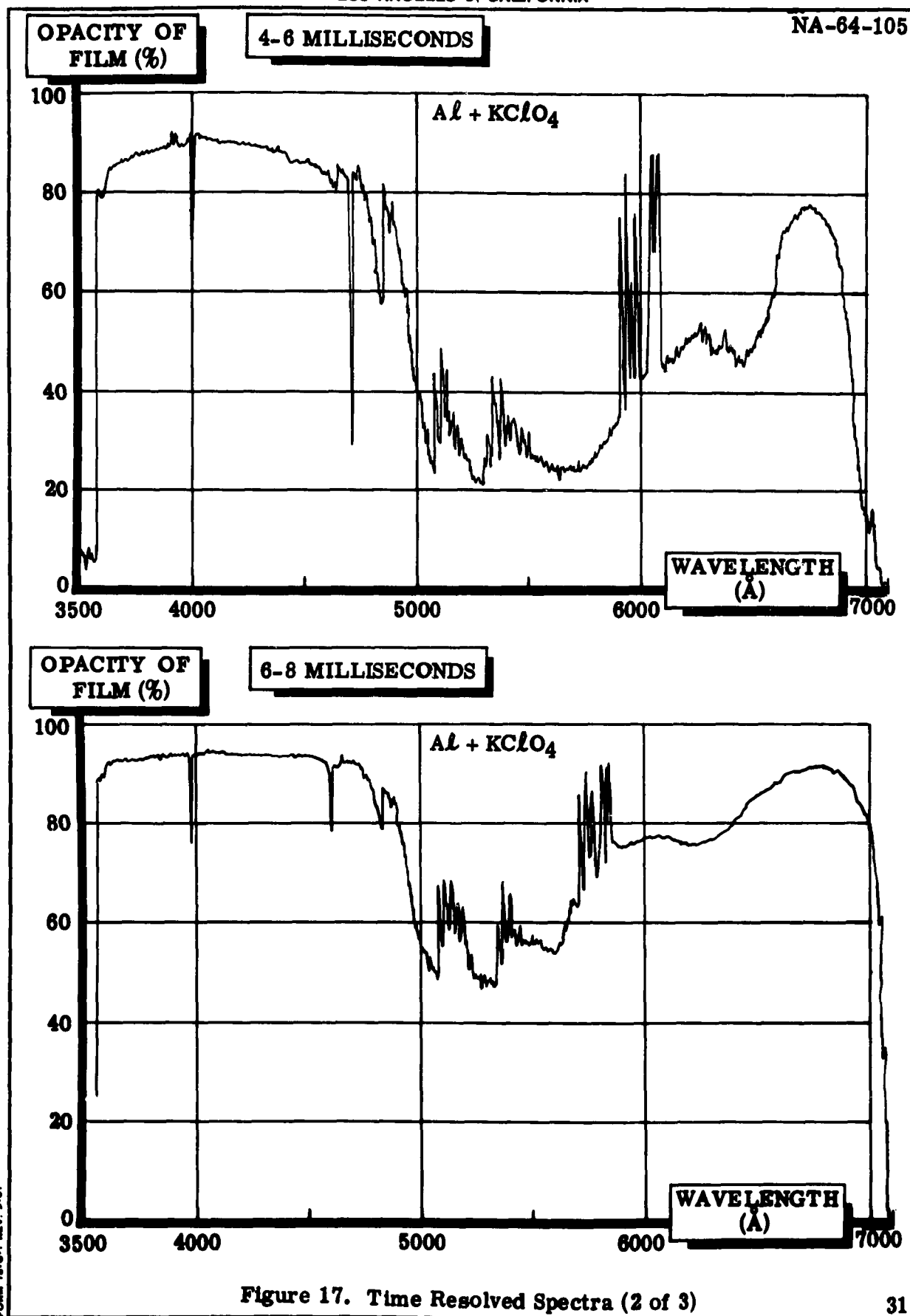
Figure 17. Time Resolved Spectra (1 of 3)
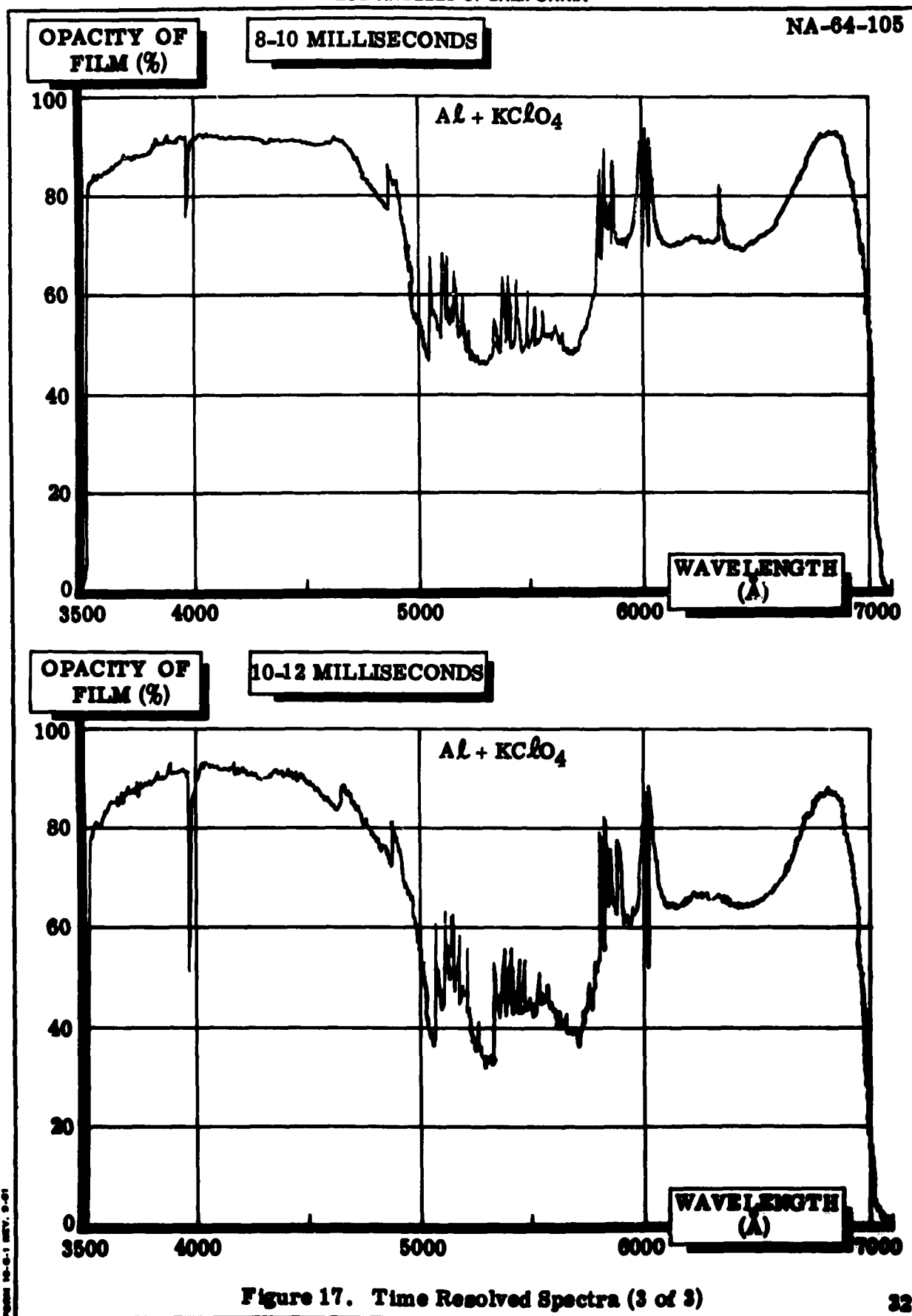
NA-64-105

OPACITY OF FILM (%)

4-6 MILLISECONDS

$A\ell + KC\ell O_4$

WAVELENGTH (Å)

OPACITY OF FILM (%)

6-8 MILLISECONDS

$A\ell + KC\ell O_4$

WAVELENGTH (Å)

Figure 17. Time Resolved Spectra (2 of 3)

FORM 18-G-1 REV. 9-61

Figure 17. Time Resolved Spectra (3 of 3)

Measurement of Emissivity and True Temperature - Single-double path measurements: Temperatures determined by phototubes sighted on a radiation source are brightness temperatures, or, the temperature at which a blackbody would be an equivalent radiation source. Measuring the true temperature of a source requires that the emissivity be known. There is evidence from the brightness temperature data taken thus far at both large pressures and at one atmosphere, that the emissivity of the luminous cloud is low. If this is indeed the case, it would indicate that additives to modify the emissivity should be given consideration.

To measure the true temperature of the flash reaction an apparatus was set up to perform single-double path measurements. The set up is shown in Figure 18. The arrangement is similar to that for measuring brightness temperature except that a spherical mirror and a light chopper have been added behind the flash. The spherical mirror is set at a distance from the chemical reaction equal to its radius of curvature so as to form an image at the focal point of the lens system. The phototube now responds to an alternating signal consisting first of radiation directly from the flash and then, when the chopper opens the optical path to the mirror, radiation directly from the flash plus radiation from the flash that has been attenuated by reflection from the mirror and by traveling through the luminous cloud. The equations for the single-double path process can be easily set down and solved if light scatterings is neglected. (The left hand side of the equations is Wien's approximation to Plank's law).

Single Path

$$\left[\frac{c_2 \lambda^{-5}}{e^{c_1/\lambda T_1}}\right] = \sigma T_F^4 \left(1 - e^{-\gamma_a L}\right) \tag{1}$$

Double Path

$$\left[\frac{c_2 \lambda^{-5}}{e^{c_1/\lambda T_2}}\right] = \sigma T_F^4 \left(1 - e^{-\gamma_a L}\right)\left(1 + \rho e^{-\gamma_a L}\right) \tag{2}$$

Solving the two equations for the two unknowns, E_F and T_F, it is found that

$$\mathcal{E}_F = \left(1 - e^{-\gamma_a L}\right) = 1 - \frac{exp\left[-c_2/\lambda(1/T_2 - 1/T_1)\right] - 1}{\rho_m} \tag{3}$$

and

$$\tag{4}$$

$$T_F = 1/\left[1/T_1 + (\lambda \ln E_F)/c_2\right]$$

Scattering of light may be of importance to the emissive properties of the cloud and can make the determination of emissivity much more difficult. The simplest analysis that can be made of a situation involving light scattering would be to assume that all scattered radiation leaves the optical path to the sensor and negligible light is scattered into the path. In this case the equations are:

Single Path

$$\left[\frac{c_2 \lambda^{-5}}{e^{c_1/\lambda T_1}}\right] = \sigma T_F^4 \left(\frac{\gamma_a}{\gamma_a + \gamma_s}\right)\left[1 - exp\left\{-(\gamma_a + \gamma_s)L\right\}\right] \tag{5}$$

43

NA-64-105

SPHERICAL MIRROR

LIGHT CHOPPER

TACHOMETER SIGNAL
FROM PHOTODIODE
TO CRT

FLASH

LENS AND LIGHT SHIELD

NARROW BAND FILTER

PHOTOTUBE

CRT
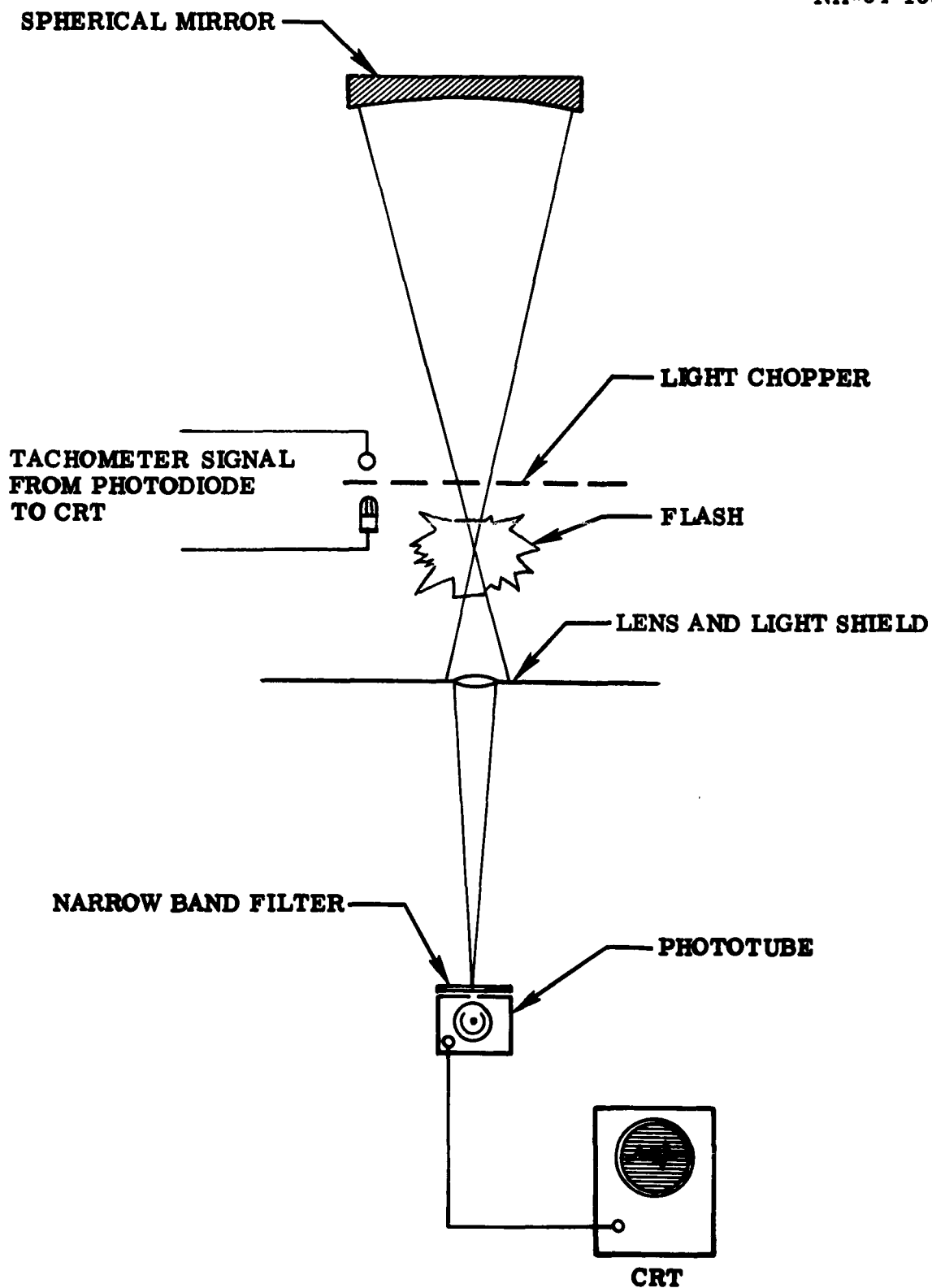
Figure 18. Single-Double Path Apparatus

34

Double Path

$$\left[\frac{c_2\lambda}{e^{c_1/\lambda T_2}}\right]^{-5} = \sigma T_F^4 \left(\frac{\delta_a}{\delta_a+\delta_s}\right)\left[1-exp\left\{-(\delta_a+\delta_s)L\right\}\right]\left[1+\rho\,exp\left\{-(\delta_a+\delta_s)L\right\}\right] \qquad (6)$$

These equations cannot be solved rigorously because they contain three unknowns δ_a, δ_s, and T_F. Comparing the equations 1 and 2 and 5 and 6 it can be seen that the solution for E_F from equations 1 and 2 diminished by $\delta_a/(\delta_a+\delta_s)$ when equations 5 and 6 are used (the change from · to · in the exponential terms is of no consequence numerically). The equations 5 and 6 are approximations to the rigorous solution of the multiple scattering problem and are valid when $\delta_a \gg \delta_s$ (3). The relative size of δ_a and δ_s, the absorption and scattering cross sections, can be rigorously calculated for a certain wavelength by use of Mie's theory. One must know, however, the complex refractive index of the material and the particle sizes. Neither of these quantities is known.

Single and double path measurements have been made during flashes of Al, Zr, and Hf with $KClO_4$ at the wavelengths 4500Å, 5000Å, and 6000Å. With a chopper frequency of 1000 to 2000 cycles per second there was no great difficulty in distinguishing the alternating signal output of the phototube from random variations in the light output of the flash process. A typical phototube response during single-double path measurements is shown in Figure 19 as displayed on a CRT. The lower trace is the chopper frequency detected by a phototransistor --- light source combination described in connection with the time resolved spectra.

Since the flashes investigated were set off on a flat plate, the optical path length of the luminous cloud as well as the mass of material in the optical path are unknown. The results of these experiments could not be used for the prediction of emissivity of radiating clouds of similar particles viewed at other optical depths. As stated before, the object was merely to measure the true flash temperature.

It was usually observed that the opacity of the luminous cloud increased with time and in some cases became completely opaque (radiation from the reflecting mirror didn't penetrate the cloud) during the latter portion of the flash.

Some experiments were performed in which the phototube and lens was set at a slight angle ($\sim 20°$) to the direction of the reflected light from the spherical mirror -- this was done to see if scattered radiation from the background source could be detected. None was detected. The solid angle viewed by the phototube was very small (0.00464 steradians) and scattered radiation would have been difficult to pick up and distinguish from radiation directly from the flash.

Because of the small solid angle viewed by the phototube it appears reasonable to expect that a narrow beam of radiation from a source placed behind the flash would obey the Bouger-Lambert law: $I_{out} = I_{in}\,exp\left\{-(\delta_a+\delta_s)L\right\}$.

The data gathered using the single-double path technique are compiled in Table II along with the calculated adiabatic flame temperature of the metals reacting with $NaClO_4$. Potassium was not on the data tapes used in the computations). The emissivities and temperatures tabulated were calculated using

Table II

MEASURED "EMISSIVITY" AND "TRUE TEMPERATURES"
FROM SINGLE-DOUBLE PATH EXPERIMENTS

	4500 Å		5000 Å		6000 Å	
	E	T	E	T	E	T
Hf - $KClO_4$	0.86	- 3640°K	0.628	- 3655°K	0.9	- 3590°K
	0.90	- 3625	0.81	- 3720		
	0.73	- 3710	0.83	- 3720		
Al - $KClO_4$	0.67	- 3390	0.86	- 3310	0.80	- 3307
Zr - $KClO_4$	0.6	- 3670			0.79	- 3390
					0.73	- 3435
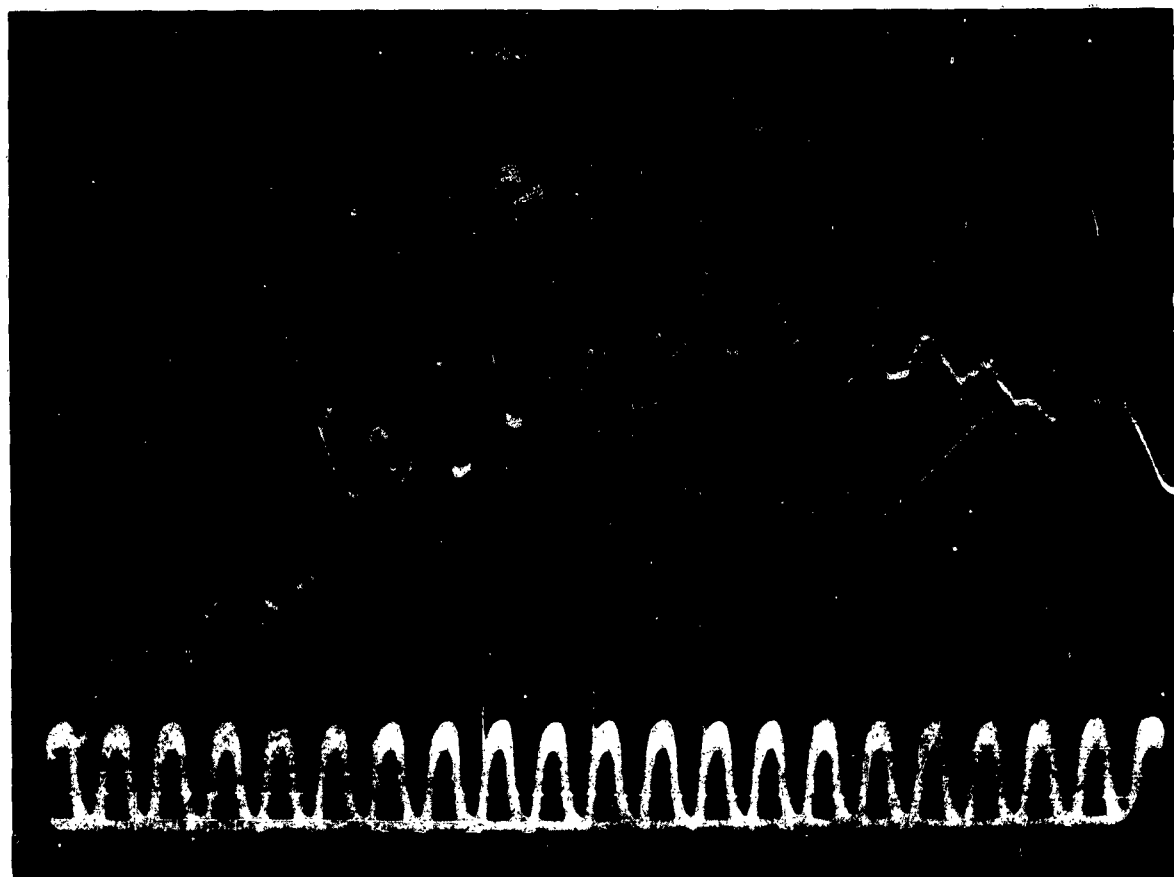
TIME (2 MSEC/DIV) ⟶

Zr-KClO_4 FLASH

$\lambda = 5900 - 6100\mathring{A}$

Figure 19. Phototube Output Single-Double Path Measurement

equations 1 and 2, that is, using the assumption that $\delta_a \gg \delta_s$. There is some doubt about the importance of scattering and the matter will have to be examined more fully in the future.

Emission Spectra - Emission spectra have been taken of the reaction of stoichiometric mixtures of $KClO_4$ and aluminum, zirconium, hafnium, lanthanum and neodymium powder. The spectra were taken using the Bausch and Lomb 1.5 meter spectrometer with Kodak 103F film and covered the region from 3660Å to about 7000Å. Most of the band structures observed have been identified as being due to metal oxides (AlO, ZrO, HfO, LaO) using the tabulation of Pearse and Gaydon (2). The spectra are shown in Figures 20 and 21 with the metal oxide bands labeled. The band structure of HfO has not been analyzed and only the location of prominent band heads listed by Pearse and Gaydon (2) are pointed out in that figure.

Additives - Neodymium was included in a list of possible reactants primarily because it was expected that the rare earths might emit in the region where rare earth dopants in the lattices of lasers would have absorption bands. Hopefully, rare earth additives would modify or tailor the spectral emission characteristics of the chemical flash. Spectra of the $Nd-KClO_4$ flash reaction were taken and found to contain only continuum radiation from solid particles and a number of fine lines attributable to Nd vapor or impurities (see Figure 22 film II exposure B). None of the NdO emission bands listed by Pearse and Gaydon (2) could be identified. There was no evidence of higher emission in spectral regions where Nd in glass lasers can be pumped.

Neodymium addition was tried in zirconium and aluminum powder flashes to see if the emissive characteristics of the flash reactions could be tailored. The spectra taken appear in Figure 22. It was found that small amounts of Nd in Zr resulted in a large reduction or disappearance of the band structure of ZrO; the emission is mostly continuum and resembles that of the $Nd-KClO_4$ flash in its lack of band structure. Also shown in Figure 22 is the spectrum of $Al-KClO_4$ with and without Nd addition. Addition of about 20 per cent by weight of $Nd-KClO_4$ to $Al-KClO_4$ did not obscure the AlO band structure and produced some identifiable band structure of NdO extending from 5971Å to 6629Å. There also appeared to be a slight enhancement of continuum radiation in the red; this enhancement however, is not in the Nd glass laser pumping bands.

Probably the boiling point of ZrO_2 is high enough so that additives resulting in a lowering of the flame temperature greatly reduce the amount of ZrO vapor present. This colder burning mixture will then exhibit a much reduced oxide band structure. The aluminum burns mostly in the vapor phase and the flame temperature of $Al-KClO_4$ mixture is closer to the measured temperature of $Nd-KClO_4$ so that the cooling effect of Nd is less. The NdO bands are not visible in the zirconium metal flashes because the continuum radiation is intense enough to obscure them.

Some spectra have been taken of flash reactions of Al and $KClO_4$ to which $BaNO_3$ had been added. This was done because $BaNO_3$ has been reported by Picatinny to enhance the brightness temperature of $Al-KClO_4$ flash bombs. The $BaNO_3$ is itself an oxidizer and is supposed to be an effective catalyst for $KClO_4$ decomposition to KCl (4). An emission spectrum of a 40 per cent Al-30 per cent $KClO_4$-30 per cent $BaNO_3$ flash is shown in Figure 21 and can be compared with the

Figure 20. Emission Spectra of Metal - KClO₄ Flashes

SPECTRUM OF La-KClO$_4$ FLASH (32 μ SLIT)
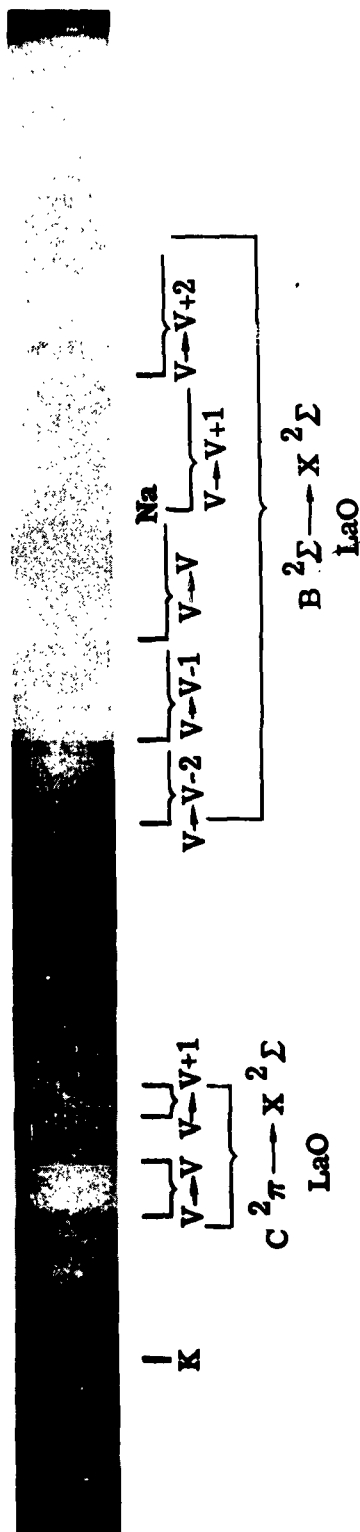
SPECTRUM OF 40% Al- 30% KClO$_4$ - 30% Ba NO$_3$ FLASH (10 μ SLIT)
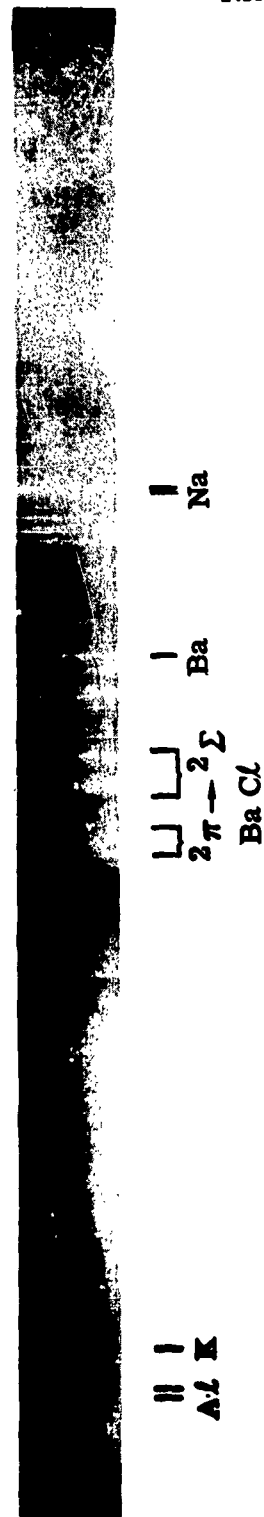
Figure 21.   Emission Spectra of Metal - KClO$_4$ Flashes
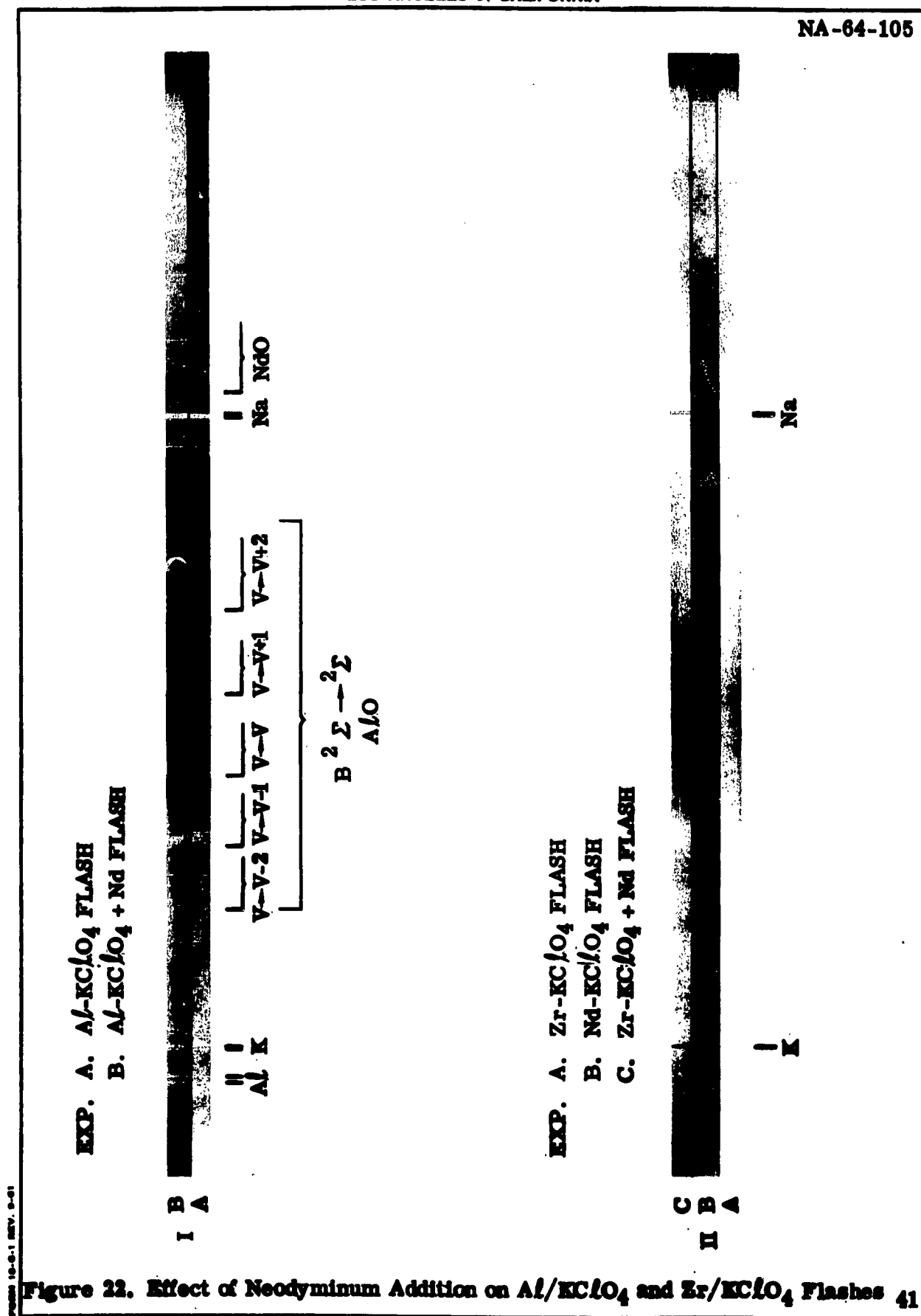
40

Figure 22. Effect of Neodyminum Addition on $Al/KClO_4$ and $Zr/KClO_4$ Flashes

spectrum of Al-KClO$_4$. The main difference between the two is the band structure of BaCl centered at 5136, 5139.9, 5240.5 and 5320.8Å (BaO bands are not visible). The increased brightness temperature might be attributed to the added emission of the BaCl bands, but is more likely due to increased reaction rates because of the catalysis of KClO$_4$ decomposition.

Section IV

NONEQUILIBRIUM STUDIES

Equilibrium is defined as the condition for which no potential exists for changing the energy distribution. All other conditions are nonequilibrium conditions.

By the definition of nonequilibrium, it is seen that many different energy modes may be in nonequilibrium. Radiation is generally not in equilibrium; it is usually deficient in energy. Chemical equilibrium generally does not exist unless the system is at high temperature; the chemical system usually has an excess of energy. Electronic, vibrational, rotational, and kinetic energy modes are generally in equilibrium except under low pressure conditions. Our problem is to take the chemical nonequilibrium and convert the excess energy to radiation of a specified frequency range.

To convert chemical energy to radiation, many different techniques are available. These techniques take the energy of the chemical system and transform it one or more times to finally obtain radiation. Each energy transformation is limited by the laws of radiation and thermodynamics, which allows us to put limits on the efficiency of transformation of the proposed techniques.

The occurrence of nonequilibrium and techniques of use are analyzed for guidance in the pumping program.

Theoretical Bases

The bases for an analysis of the radiation and thermodynamic laws. In particular the considerations of interest here are: blackbody radiation (5), emissivity (5), theoretical flame temperatures (6), entropy (7), and equilibrium energy distribution (8). Since these topics are covered adequately in the literature, only the final equations are given.

Black body radiation is described by Planck's equation

$$\rho_\nu^o(T) = 8\pi h \nu^3 / [exp(hc\nu/kT) - 1]$$

where ρ_ν is energy density at the frequency ν (frequency in wave numbers per cm). The superscript zero indicates blackbody. Defining the radiancy

$$\mathcal{R}_\nu^o = c^2 \nu^2 \rho_\nu^2 / 4$$

Integrating over the frequency gives

$$R^0 = \sigma T^4$$

for the total radiation energy for all wave lengths.

The emissivity is defined as

$$R = \varepsilon R^0$$

or

$$R_\nu = \varepsilon_\nu R_\nu^0$$

for the total emissivity ε or the spectral emissivity ε_ν. The emissivity, ε, reflectivity, r, and scattering coefficient, s, are related

$$1 = \varepsilon + r + s$$

or

$$1 = \varepsilon_\nu + r_\nu + s_\nu$$

Often $s = s_\nu \approx 0$ and the scattering is ignored.

Theoretical flame temperatures are calculated by 1) mass balance equations, 2) enthalpy balance equation, pressure balance equation, and 4) equilibrium constants. These equations are all that are needed to specify the system. Since equilibrium is assumed, complete combustion is assumed. Since an enthalpy balance is assumed, an adiabatic system is assumed. (While not used, the flame temperature at constant volume can be calculated by replacing the enthalpy by the internal energy and pressure by density.)

The entropy is important for determining the limits on energy conversion if an isentropic process occurs, the equilibrium conditions hold. Thus, in an isentropic radiation process, the blackbody limit is imposed. The entropy is defined

$$dS = dS_r + dS_i$$

$$= \frac{dQ}{T} + \frac{dQ}{T}$$

where r indicates reversible and i irreversible Q is an artificial variable to make both terms formally the same. The definition of dQ is

$$-dQ = dU\big|_{s,v}$$

In other words, an irreversible change is accompanied by a decrease in internal energy. The implications of this statement are amplified during the discussion on tapping.

The Boltzman energy distribution is given as

$$m_i = N \omega_i \exp(-\varepsilon_i/kT) / P.F.$$

44

where n_i is the population of state i, ω_i is the statistical weight of state i, and E_i is its energy level. Ignoring negligible quantum effects, this gives the equilibrium distribution. Conversely given n, a temperature for the state is defined. The energy levels are for any mode--kinetic, rotational, vibrational, or electronic.

Nonequilibrium State

Since nonequilibrium is defined as not at equilibrium, there are many and varied nonequilibrium conditions. In a nonequilibrium condition, there is a driving force or potential that will tend to equilibrate the systems. To use the nonequilibrium potential for laser pumping, potential must be converted to radiation in a spectral band. This is the objective of this study.

Nonequilibrium exists as frozen composition (as mixing zirconium and $KClO_4$ at room temperature), radiative nonequilibrium, excess excitation of energy levels (often occurs because of chemi-excitation), hot spots, and underexcited energy levels (giving a higher kinetic temperature). Since hot spots and underexcitation are characteristic of low pressure systems (and hence poor radiative systems), these modes of nonequilibrium are not discussed further. In addition frozen composition is the typical for chemical reactions. The only phase of interest to this study is the energy output and combustion efficiency. Thus the nonequilibrium aspect is not discussed.

Radiation

There are a number of problems associated with radiation. The ones of interest in this study are emissivity, optical depth, and chemiluminescence. While important, emissivity and optical depth are not discussed in this section. Chemiluminescence is the basis for tailoring and tapping energy of chemical reactions. In a chemical reaction, the energy released goes into kinetic, rotational, vibrational, and electronic energy. Generally, the energy goes to exciting the molecule rather than kinetic energy as:

$$O + H + M \longrightarrow OH^* + M^*$$
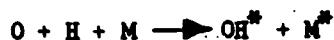
Thus easily excited species are much more effective third bodies than monatomic species. Since excitation is the primary path of a reaction, our problem is to tap this energy before it converts to kinetic energy.

The temperature of the excited state can be calculated from the distribution

$$E_i/kT = \ln(N/n_i)$$

This temperature (which is not the kinetic temperature) controls the radiation equilibrium--assuming no absorption in the surrounding gas. As such, it appears that the black body radiation limit for the radiating gas is unimportant. A more serious problem can occur from a mantle of

nonexcited gas surrounding the radiating gas.

Overexcitation

Excitation can occur by thermal excitation, excitation transfer, and chemical reaction. In thermal excitation, the excitation is in equilibrium with the kinetic temperature. This produces the normal excitation for comparison. It becomes overexcitation only when the kinetic temperature decreases rapdily--which does not occur in our system. In excitation transfer, the excitation energy is transferred from one specie to another. This is the mechanism for tailoring radiation, but overexcitation is not produced this way, only transferred. Chemical excitation is the only method for production of overexcitation in our system. In a chemical reaction, the chemical energy is converted into excitation energy and kinetic energy. The usual conservation laws (mass, momentum, angular momentum, spin, and energy) hold for collision in which a chemical reaction occurs (9). Since momentum is a vector quantity, it is possible that all the energy can be converted to kinetic energy by a superelastic collision. The cross section for the various collisions, must be obtained to give the ratio of excitation to kinetic energy. However, in almost every reaction studied for excitation, it has been found. This is the source of nonequilibrium excitation in our system.

Techniques

In tapping or tailoring radiation, a high emissivity material is used as a dopant. In tailoring the radiation, the emission is raised toward the black body limit for the kinetic temperature. In tapping, the energy of excitation is converted to radiation. If the excitation is at an effective temperature higher than the kinetic temperature, the radiation can be above the black body limit for the kinetic temperature. The limiting temperature in all cases is the effective temperature of the pertinent process. (Unfortunately, this is many times the cool outer portions of the combustion.)

As dopants, metals, salts (with strong dipoles), and fluorescent solids are considered. If the fluorescent solid will work, it appears to be the best choice. The energy of condensation should be easily tapped. The emitted radiation is less likely to be reabsorbed, and most fluorescents are radiators. Possibly it will not be able to take the conditions of the combustion. Since the total combustion time is short, there is a chance that the fluorescent solid can survive.

If the fluorescent solid will not work, metals and salts will be tried as dopant. Both are strong gaseous radiators. There is a possibility that, since the condensation is the energetic reaction, gaseous species will not be able to tap the system. Thus an experimental program is essential for testing the systems.

46

Candidate Systems

Calculations were run for aluminum and potassium perchlorate, and for zirconium and potassium perchlorate. Adiabatic flame temperatures for the two systems are about 5000°K and 5500°K respectively at 68 atmospheres pressure. This gives a radiation intensity of 2.31×10^{-2} e/ρ and 3.59×10^{-2} e/ρ kcal/gm in the visible. (The density converts to mass from the area radiation to make the units comparable to the excess energy at lower temperatures.)

If we allow the systems to combust at one atmosphere at a temperature sufficiently high for good combustion (2700K for Al and 3000 for Zr), there is considerable excess energy. It amounts to 5.4 kcal/gm for the aluminum and 0.99 kcal/gm for zirconium.

Looking at the thermochemical data, only beryllium, boron, and lithium appear to be comparable to aluminum. This easiest system to handle is one of the best.

Most metals are good radiators as are fluorescent materials. Thus, the main interest is to select the correct radiation bands. Examples of metals are Ti, Y, Ag, Cu, Ba, Tl, and Hg. Since we are interested in the metal and not a compound, the metal should be relatively inactive. All except barium in the above list are less active than aluminum.

Typical phosphors that radiate in the correct spectral region are Zn_2SiO_4: Mn, ZnS: Ag: Cu, Zn_3 $BeSi_5$ O_{19}: Mn, and MgS: Sb. In addition, a short persistence and high saturation density are desired. Of the listed fluorescent materials, ZnS: Ag: Cu has a long persistence.

Salts that have large dipole moments are usually good radiators. Since transition probabilities are hard to come by, initial screening is by dipole moments. In general, large dipole moments occur in polyatomic molecules--which have only a limited spectral analysis. Thus the screening on molecules will be the heavy metal chlorides and fluorides. It is hoped that augmentation will occur with these salts.

NA 64-105

Section V

REFERENCES

1. Kodak Plates and Films for Science and Industry, Eastman Kodak Company, 1962.

2. Pearse, R.W.B. and Gaydon, A.G., "The Identification of Molecular Spectra", 2nd Ed. Revised. John Wiley and Sons Inc. (1950).

3. Stull, R.V., and Plass, G. N., J. Am. Opt. Soc., 50, 121-129 (1960).

4. Hogan, V.D. and Gordon, S.J. Phys. Chem., 62, 1433-5 (1958).

5. Penner, S.S., "Quantitative Molecular Spectroscopy and Gas Emissivities," Addison-Wesley, Reading, Mass., 1959, Chapter 1.

6. Thompson, R. J., "High Temperature Thermodynamics and Theroetical Performance Evaluation of Rocket Propellants," Rocketdyne Report, June 1959.

7. I Prigogine and Defay, R. "Chemical Thermodynamics", John Wiley, New York, 1954, Chapter 1.

8. Fowler, R., and Guggenheim, E.A., "Statistical Thermodynamics", Cambridge University Press, Cambridge Eng., 1939, Chapter 5.

9. Hirshfelder, J, Curtiss, C.F., and Bird, R.B., "Molecular Theory of Gased and Liquids," John Wiley, New York, 1954, Chapter 7.6.

PROGRAM CONTRIBUTORS

Dr. J. M. Gerhauser   Rocketdyne Division

Mr. J. J. Pierro   Los Angeles Division

Mr. G. R. Schneider   Rocketdyne Division

Mr. J. A. Macken   Los Angeles Division

Mr. P. N. Palanos   Los Angeles Division